Organometallics 2017, 36, 3692−3708. doi: 10.1021/acs.organomet.7b00488

Expanding the Family of Hoveyda-Grubbs Catalysts containing Unsymmetrical NHC Ligands

Veronica Paradiso,[†] Valerio Bertolasi,[‡] Chiara Costabile,[†] Tonino Caruso,[†] Michał Dąbrowski,[‖] Karol Grela[‖] and Fabia Grisi*[†]

[†]Dipartimento di Chimica e Biologia "Adolfo Zambelli", Università di Salerno, Via Giovanni Paolo II 132, I-84084 Fisciano, Salerno, Italy

[‡]Dipartimento di Chimica and Centro di Strutturistica Diffrattometrica, Università di Ferrara, Via L. Borsari 46, I-44100 Ferrara, Italy

‖ Biological and Chemical Research Centre, Faculty of Chemistry, University of Warsaw, Żwirki i Wigury 101, 02-089 Warsaw, Poland

Corresponding author: fgrisi@unisa.it

Abstract

A series of Hoveyda-Grubbs' second generation catalysts containing *N*-alkyl/*N'*-aryl N-heterocyclic carbene (NHC) ligands were synthesized and investigated in representative olefin metathesis reactions. Steric perturbations of unsymmetrical NHCs were achieved through modulation of the hindrance of alkyl (neopentyl, neophyl, cyclohexyl) and aryl (2-isopropylphenyl, mesityl) substituents at the nitrogen atoms in combination with different backbone configuration (*syn* or *anti*). The NHC substitution patterns strongly influence stability and reactivity of corresponding complexes. In general, complexes bearing an *anti* NHC backbone are more stable and more active than their corresponding *syn* isomers. In both the series, the presence of bulky, highly branched *N*-alkyl groups tends to give reduced catalytic differences between *syn* and *anti* isomers, whereas the nature of the *N*'-aryl substituent (2-isopropylphenyl or mesityl) gave rise to different activity and/or

Organometallics 2017, 36, 3692−3708. doi: 10.1021/acs.organomet.7b00488

selectivity. Of note, *N*'-mesityl catalyst with *anti* backbone was found to be highly competent in the ethenolysis of ethyl oleate, achieving up to 90% selectivity for the formation of terminal olefins.

Introduction

The last few years have seen significant advances in the chemistry of olefin metathesis,[1] mostly due to the development of easy-handling, highly efficient NHC-based ruthenium catalytic systems (second generation catalysts),[2] which have found successful applications in the synthesis of natural products and pharmaceuticals as well as in the production of fine chemicals and oleochemicals.[1,3] Catalytic behavior of this class of ruthenium complexes can be easily modulated through judicious modification of the stereoelectronic properties of the NHC ligand. This feature has allowed for the development of a huge number of catalysts with different NHC architectures,[4] including unsymmetrical NHC (uNHC) frameworks, whose fascination lies mainly in the possibility that they offer to strongly differentiate the steric bulkiness around the metal, hence influencing catalyst activity and selectivity.[5] In this view, the catalytic potential of ruthenium complexes coordinated with uNHCs, especially those presenting one aliphatic and one aromatic amino side group,[6] has been investigated by many researchers (e.g. **1-6**, Chart 1**)**. Successful results in specific metathesis applications, such as asymmetric reactions,[5f,7] synthesis of alternating copolymers,[8] selective formation of cyclic oligomers,[9] ethenolysis reactions,[6d,8b] *Z*-selective metathesis transformations[5e,f,10] and diastereoselective ring rearrangement metathesis[6e,11] have been achieved.

Organometallics 2017, 36, 3692−3708. doi: 10.1021/acs.organomet.7b00488

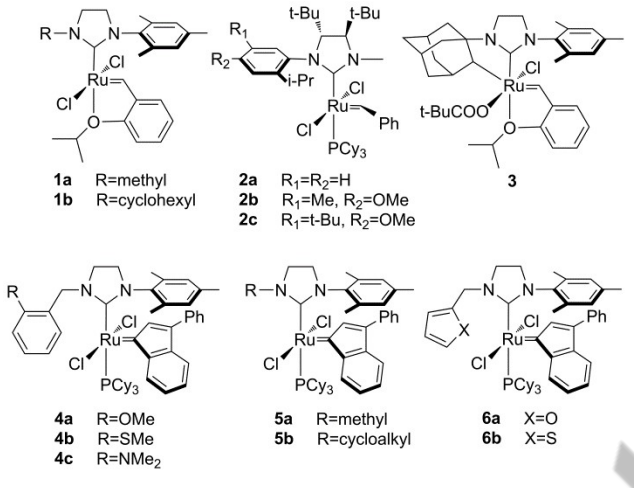

Chart 1. Selected examples of ruthenium catalysts with unsymmetrical NHCs

We have recently proposed an additional strategy for tuning the catalytic properties of this class of complexes, based on the introduction of substituents on the backbone of unsymmetrical NHC moieties in a precise stereochemical arrangement (*syn* or *anti*) (**7-10**, Chart 2). Through this structural modification, metathesis ruthenium complexes showing different catalytic behavior depending on the NHC backbone configuration (*anti* or *syn*) and on the bulkiness of the *N*-alkyl substituent (*N*-cyclohexyl vs *N*-methyl) were obtained.[12]

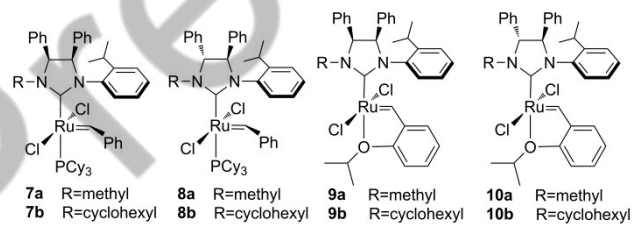

Chart 2. Ruthenium catalysts with backbone substituted uNHCs

To further investigate the impact on catalyst properties of unsymmetrical NHCs that combine stereogenic centers on the backbone with differently encumbered *N*-alkyl/*N'*-aryl substituents, we focused our attention on the development of new Hoveyda-Grubbs type complexes (**11a-c** and **12a-c**, Chart 3) with modified *N*-substituents. In particular, *syn* and *anti* NHC backbone substituted complexes possessing an *N*-neopentyl or neophyl moiety mixed with an *N*'-2-isopropylphenyl

Organometallics 2017, 36, 3692−3708. doi: 10.1021/acs.organomet.7b00488

group (**11a,b** and **12a,b**), as well as the analogues having *N*-cyclohexyl/*N'*-mesityl substituents (**11c** and **12c**), were prepared and structurally characterized. The catalytic performances of **11a-c** and **12a-c** were evaluated in standard metathesis reactions and compared with those of previously reported catalysts **9b** and **10b**, presenting the most significant reactivity difference between *syn* and *anti* isomers. Furthermore, the catalytic potential of all these complexes was explored in a specific metathesis application such as ethenolysis of fatty acid esters, whereas the enantioselective ability of chiral catalysts **12a-c** was investigated in model asymmetric ring-closing metathesis (ARCM) and asymmetric ring-opening cross-metathesis (AROCM) reactions.

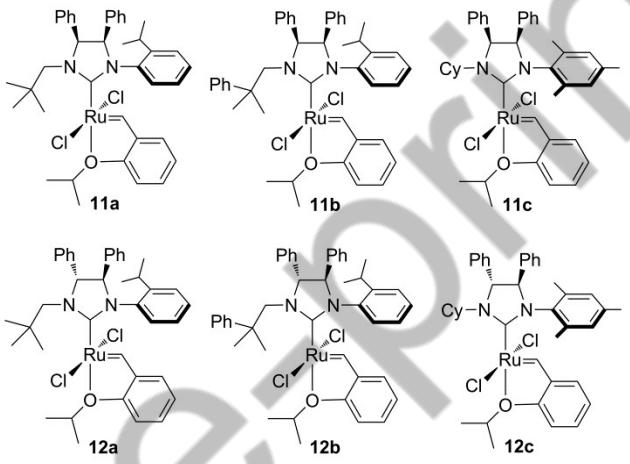

Chart 3. New ruthenium catalysts bearing uNHCs with different backbone configuration. Catalysts **11a-c** are racemic mixtures (only one of the enantiomers is depicted), while **12a-c** are enantiopure.

Results and discussion

Synthesis and characterization of complexes 11a-c and 12a-c

The new complexes **11a-c** and **12a-c** were easily obtained following the synthetic procedures illustrated in Schemes 1 and 2, respectively.[12a] Diamines **13**, **14** and **17** were obtained from the commercial *meso*- or (*R,R*)-1,2-diphenylethylenediamine by cross-coupling with 2-isopropylbromobenzene or 2-bromomesitylene and subsequent reductive amination of the appropriate aldehyde or ketone (50-79% yields), whereas diamine **18** was prepared installing first

Organometallics 2017, 36, 3692−3708. doi: 10.1021/acs.organomet.7b00488

the cyclohexyl and then the mesityl group (51% yield) on the nitrogen atoms of the starting (*R,R*)-1,2-diphenylethylenediamine. After cyclization of the so-obtained diamines in the presence of triethylorthoformate and ammonium tetrafluoroborate, the resulting NHC salts (71-90% yields) were deprotonated in situ with $(CF_3)_2(CH_3)COK$ and reacted with $RuCl_2$(=CH-*o*-*i*PrO-Ph)(PCy_3) (**HGI**) to afford the desired complexes **11a-c** and **12a-c** as air and moisture stable solids, in yields ranging from moderate to good (45-70%). It should be underlined that complexes **11a-c** are racemic mixtures, while **12a-c** are enantiopure.

Scheme 1. Synthesis of ruthenium complexes **11a-c**.[a]

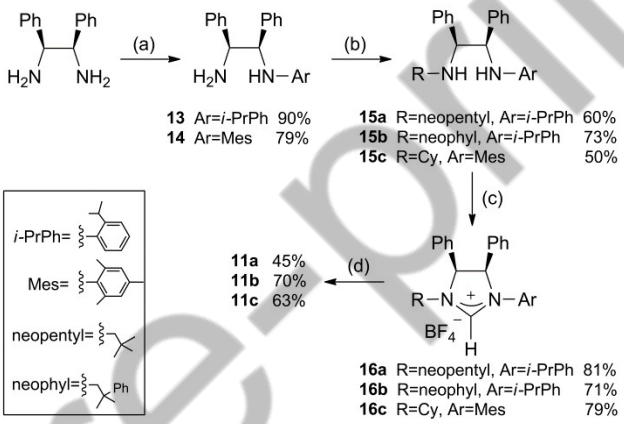

[a]Reaction conditions: (a) *meso*-1,2-diphenylethylenediamine, 2-isopropylbromobenzene (for **13**) or 2-bromomesitylene (for **14**), $Pd(OAc)_2$, NaOtBu, BINAP, toluene, 100 °C, 12 h; (b) 1: $R(CH_3)_2CCHO$ (R=Me, Ph) or cyclohexanone, CH_2Cl_2, molecular sieves, RT, 48h (for **15a**) or 5 days (for **15b** and **15c**); 2: $NaBH_4$, CH_3OH, RT, 3.5 h; (c) NH_4BF_4, $CH(OEt)_3$, 135 °C, 2 h (for **15a** and **15c**) or 8h (for **15b**); (d) $(CF_3)_2CH_3COK$, **HGI**, toluene, 65°C, 2.5h.

Organometallics 2017, 36, 3692−3708. doi: 10.1021/acs.organomet.7b00488

Scheme 2. Synthesis of ruthenium complexes **12a-c**.[a]

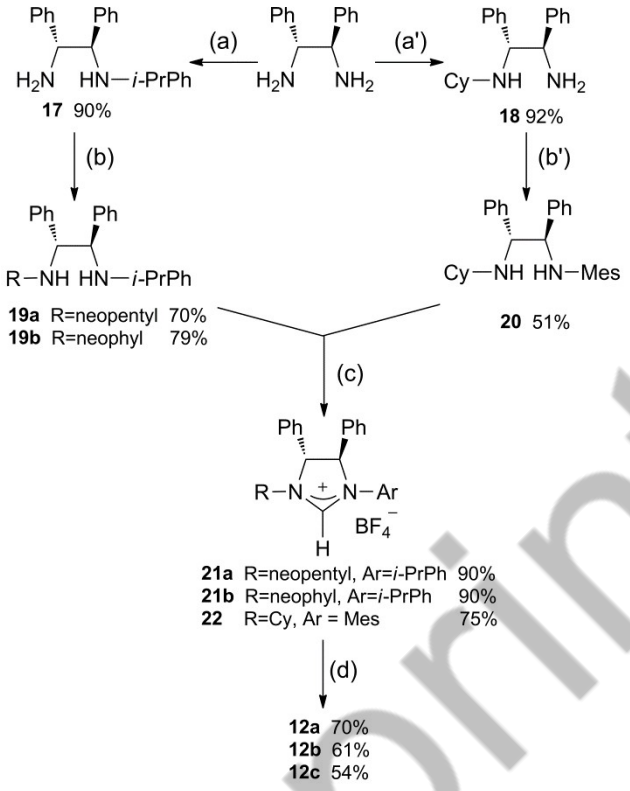

[a]Reaction conditions: (a) *(R,R)*-1,2-diphenylethylenediamine, 2-isopropylbromobenzene $Pd(OAc)_2$, NaOtBu, BINAP, toluene, 100 °C, 12 h; (a') 1: *(R,R)*-1,2-diphenylethylenediamine, cyclohexanone, CH_2Cl_2, molecular sieves, RT, 14h; 2: $NaBH_4$, CH_3OH, RT, 3.5 h; (b) $R(CH_3)_2CCHO$ (R=Me, Ph), CH_2Cl_2, molecular sieves, RT, 14h (for **19a**) or 5 days (for **19b**); 2: $NaBH_4$, CH_3OH, RT, 3.5 h; (b') 2-bromomesitylene, $Pd(OAc)_2$, NaOtBu, BINAP, toluene, 100 °C, 48 h; (c) NH_4BF_4, $CH(OEt)_3$, 135 °C, 2 h (for **19a** and **20**) or 8h (for **19b**); (d) $(CF_3)_2CH_3COK$, **HGI**, toluene, 65°C, 2.5h.

All the final products were characterized by 1D, 2D NMR techniques and ESI-FT-ICR analysis.

Crystals suitable for X-ray diffraction analysis were obtained for complexes **11a**, **11c** and **12c** and their crystal structures are shown in Figure 1**.** A selection of bond distances and angles is given in the Supporting Info (Table S2).

In all compounds the Ru center is pentacoordinated and adopts a distorted square pyramidal coordination geometry. The Cl atoms are *trans* oriented in the basal plane and the carbene C1 atom is in *trans* position with respect to the O1 oxygen of 2-*i*PrO substituent at the benzylidene ligand,

Organometallics 2017, 36, 3692−3708. doi: 10.1021/acs.organomet.7b00488

which is almost coplanar with the NHC ring, being rotated by only 8.80(8), 11.20(13) and 3.13(8)° for the three **11a, 11c** and **12c** complexes, respectively.

Compound **11a** crystallizes in the centro-symmetric $P2_1/n$ space group with the NHC phenyl groups in *cis* position with respect to C2-C3 bond. Accordingly the crystal contains a racemic mixture of both the enantiomers having opposite configurations (*SR* or *RS*) at the C2 and C3 asymmetric carbon atoms. The conformations of the substituents at N1 and N2 NHC atoms are mainly determined by short intramolecular interactions : H14b…Ru1 = 2.54 Å and H4…*Centroid* of C19/C24 phenyl ring = 2.40 Å.

Complexes **11c** and **12c** are isomers with different relative configurations at C2 and C3 atoms of NHC group. Both crystallize in the *non*-centrosymmetric *C2* space group. In **11c** the phenyl groups, bonded to C2 and C3 of NHC ring, are in *cis* position, accordingly the C2 and C3 carbons display opposite configurations: *S* and *R*, respectively. Conversely, in complex **12c** the phenyl groups at C2 and C3 are in *trans* positions and the C2 and C3 carbon atoms of NHC display the same *R* chirality. The absolute configurations could be determined reliably, from the crystallographic data, using the calculated Flack parameter[13] of 0.00(2) and -0.03(2) for **11c** and **12c** complexes, respectively.

The conformations of the substituents at the N1 and N2 of the NHC rings are controlled by short intramolecular interactions between the C4-H4 group of the benzylidene moiety and the centroid of C20/C25 phenyl ring, as well as by interactions between the C14-H14 group of the cyclohexyl substituent and the Ru atom. The C-H…π interactions between the C4-H4 group and the centroids ***C*** of C20/C25 phenyl rings are characterized by the following parameters H4…***C***(C20/C25) = 2.70 and 2.58 Å, and C4-H4…***C*** = 162 and 168°, for **11c** and **12c**, respectively. Furthermore, the short C-H…Ru interactions display H14…Ru1 distances of 2.51 and 2.50 Å, and C14-H14…Ru1 angles of 122 and 123° for complexes **11c** and **12c**, respectively.

Organometallics 2017, 36, 3692−3708. doi: 10.1021/acs.organomet.7b00488

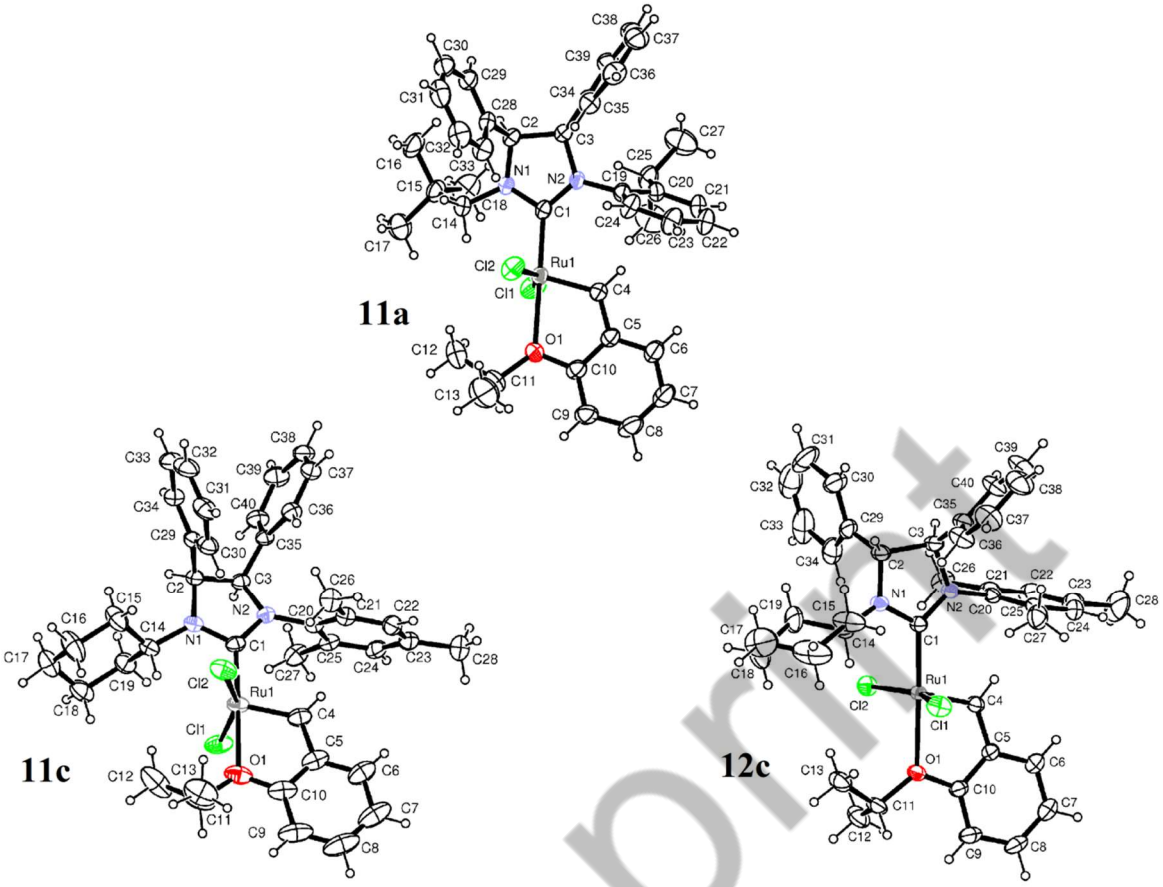

Figure 1. ORTEP[14] views of compounds **11a, 11c** and **12c** showing the thermal ellipsoids at 40% probability level.

Before investigating the catalytic behaviour of the newly developed complexes, their thermal stability was studied. C_6D_6 solutions (0.01 M) of each complex, prepared under nitrogen atmosphere and containing tetrakis(trimethylsilyl)silane as an internal standard, were heated at 60°C for one month and monitored by ^{1}H NMR spectroscopy. Stability tests performed during the first 14 days are illustrated in Figure 2. After a week, *syn* complexes **11a** and **11b** were found to be almost completely decomposed (only 4% of initial complexes remained), while their corresponding *anti* isomers **12a** and **12b** exhibited a greater stability, as they decomposed within 12 and 10 days, respectively. Moreover, decomposition rates are very similar for **11a** and **11b** but significantly different for **12a** and **12b**, suggesting a major effect of the *N*-alkyl substitution on complex stability

Organometallics 2017, 36, 3692−3708. doi: 10.1021/acs.organomet.7b00488

in the presence of an *anti* NHC backbone configuration. This is observed also for reference complexes **9b** and **10b**, where the presence of the *N*-cyclohexyl group ensures major stability with respect to catalysts **11a,b** and **12a,b**, allowing to detect, after 14 days, 32% of **9b** and 42% of **10b** unaltered. At one month, 26% of *anti* isomer **10b** still persisted, while only 8% of *syn* **9b** remained. On the other side, the presence of a more bulky *N'*-aryl substituent such as a mesityl group resulted in outstanding stability of the resulting complexes **11c** and **12c**, that indeed both showed no decomposition within one month, also proving to be more robust than the classical, commercially available **HGII** catalyst[15] bearing a symmetrically substituted NHC.[16nota]

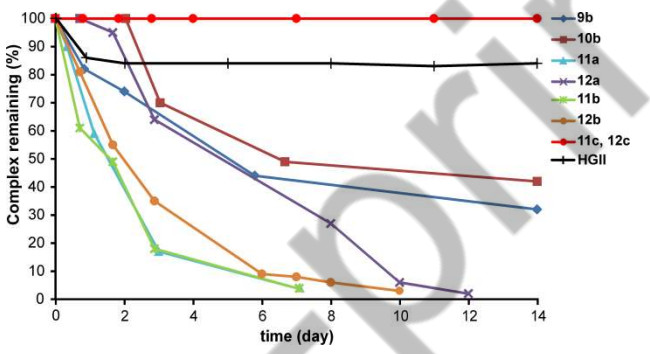

Figure 2. Thermal stability in C_6D_6 at 60°C under nitrogen of Ru complexes **11a-c** and **12a-c**. Decomposition was monitored by ^{1}H NMR spectroscopy using tetrakis(trimethylsilyl)silane as an internal standard. The lines are intended as a visual aid only.

As reported in the literature the stability of unsymmetrical catalysts is associated with the nature of NHC *N*-substituents.[6f, 17] In a recent study on NHC-Al complexes the stability was attributed to steric factors,[18] by using topographic maps and %V_{Bur} as steric parameters.[19] In this framework topographic maps (Figure 3) and %V_{Bur} of complexes **9b**, **10b** e **11a-c** e **12a-c** were calculated. Since no X-ray were available for complexes **11b**, **12a** and **12b**, we used DFT optimized structures for all complexes for topographic maps and %V_{Bur} calculation. As for complex **11b** and **12b**, it worth noting that minimum energy structures involve a partial π-stacking interaction among the phenyl substituent on the backbone and the phenyl of the neophyl group (Figure 4).

Organometallics 2017, 36, 3692−3708. doi: 10.1021/acs.organomet.7b00488

In Table 1, the percentage of undecomposed complex after 3 days, the value of $\%V_{Bur}$ representative of the most hindered quadrant ($\%V_{Bur}$ Max) and the overall $\%V_{Bur}$ are reported.

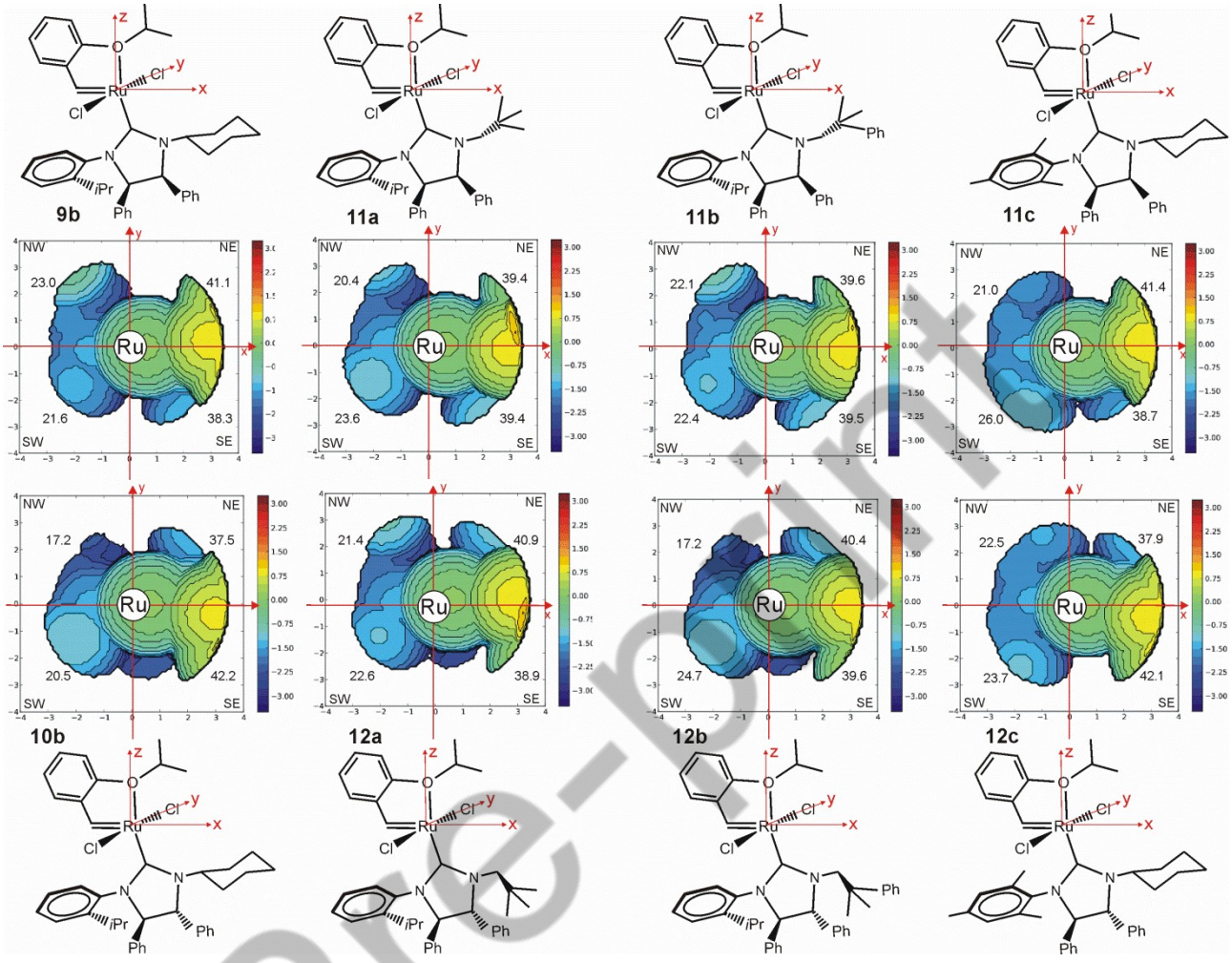

Figure 3. Topographic steric maps of **9b**, **10b**, **11a-c** and **12a-c.** The iso-contour curves of steric maps are in Å. The maps were achieved starting from minimum energy structures of complexes optimized by DFT calculations. The complexes are oriented according to the complex scheme of the corresponding map. $\%V_{Bur}$ representative of each single quadrant is reported in for each map.

Organometallics 2017, 36, 3692−3708. doi: 10.1021/acs.organomet.7b00488

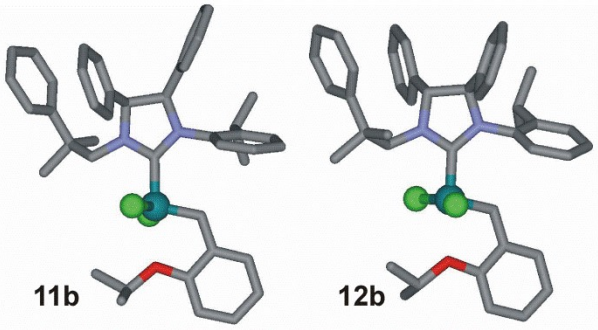

Figure 4. DFT optimized structures of complexes **11b** and **12b**.

Table 1. Percentage of undecomposed complex after 3 days, value of the %V_{Bur} representative of the most hindered quadrant (%V_{Bur} Max) and value of the overall %V_{Bur} and for **9b**, **10b**, **11a-c** and **12a-c**.

Complex	%Complex[a]	%V_{Bur} Max[b]	%V_{Bur}
11a	17	39.4	30.7
11b	18	39.6	30.9
12b	35	40.4	30.5
12a	64	40.9	31.0
9b	68	41.1	31.0
10b	70	42.2	30.5
HGII	84	42.9	32.9
11c	100	41.4	31.8
12c	100	42.1	31.5

[a] Percentage of undecomposed complex after 3 days in C_6D_6 at 60°C under nitrogen. [b]%V_{Bur} representative of the most hindered quadrant (NE or SE in Figure 3 depending on the complex shape).

According to topographic maps, higher steric hindrance is concentrated on the *N*-alkyl substituent side, that is always located far from the alkylidene. **11c** and **12c**, presenting the highest %V_{Bur}, showed also to be the most stable complexes. Nevertheless, according to the data in Table 1 the complex stability seems more correlated to the %V_{Bur} Max (representative of the most hindered quadrant). The lower the %V_{Bur} Max is, the lower the stability is shown by the complex. In order to give a more comprehensive overview, data for complex **HGII** from DFT optimization (see SI) were

Organometallics 2017, 36, 3692−3708. doi: 10.1021/acs.organomet.7b00488

also reported in Table 1 even if we did not expect a behavior in line with that of the examined catalysts due to the different nature of NHC ring substitution.

The electrochemical behavior of **9b**, **10b**, **11a-c** and **12a-c** was also investigated to gain useful information about the electron donating properties of the NHC ligand coordinated to the metal.[20] The Ru(II)/Ru(III) redox potentials derived by cyclic voltammetry are reported in Table 2.

Table 2. Redox potentials of ruthenium complexes **9b**, **10b**, **11a-c** and **12a-c** determined by cyclic voltammetry.

Complex	$\Delta E_{1/2}$ (V)[a]	(E_a-E_c) (mV)
9b	0.947	73
10b	0.960	102
11a	0.969	102
12a	0.978	112
11b	0.972	98
12b	0.976	112
11c	0.961	98
12c	0.950	83
HGII	0.860[b]	66

[a] Redox potentials determined using cyclic voltammetry in CH_2Cl_2 under nitrogen; 1mM analyte, 0.1 M NBu_4PF_6 as supporting electrolyte and 1mM octamethylferrocene as an internal standard. Scan rate: 100 mV/s. [a] Redox potential reported in the literature (ref. 20) is 0.850 V.

The values registered for complexes **9b**, **10b**, **11c** and **12c** bearing an *N*-cyclohexyl group are quite similar, varying in a range of only 3-13 mV, and no clear trend depending on the NHC backbone configuration and/or the nature of the *N*'-aryl substituent was observed. As for complexes **11a**, **11b**, **12a** and **12c** with a branched *N*-alkyl substituent, differences in redox potentials are even less significant (3-8 mV), indicating a negligible role not only of the *N*-substitution but also of the relative orientation of substituents on the backbone. On the whole, electronic properties of uNHCs coordinated to the examined complexes seem to be very little influenced by the types of substitution patterns. The lowest redox potential values, reflecting the highest electron density at the metal

Organometallics 2017, 36, 3692−3708. doi: 10.1021/acs.organomet.7b00488

center, are observed for complexes **9b** and **12c** characterized by an *N*-cyclohexyl group. Compared to **HGII** catalyst, complexes **9b**, **10b**, **11c** and **12c** are anodically shifted by 87-128 mV, underlining a lower donor ability of the corresponding uNHC ligands. This finding was already observed for ruthenium complex bearing symmetrical NHCs with phenyl groups on the backbone.[21]

Ring-Closing Metathesis (RCM) Activity Studies

The catalytic performances of **11a-c** and **12a-c** were first evaluated in RCM reactions of malonate and *N*-tosyl derivatives with different degrees of steric hindrance**.** All cyclization reactions were carried out at 60°C in C_6D_6 and monitored by ^{1}H NMR spectroscopy. The corresponding kinetic plots are shown in Figures 5-7 where the conversion-time curves previously determined for the same ring-closures promoted by catalysts **9b** and **10b**[12] are also displayed. Further details, including comparisons to commercially available **HGII** catalyst, are reported in the Supporting Info (Tables S3-S5).

In the RCM of diethyl diallylmalonate (**23**, Figure 5A), catalysts **11a**,**b** and, **12a**,**b** were able to complete cyclization in a range of 5-8 minutes, with **12a** emerging as the most efficient system, nearly equaling the best performing catalyst **10b**. However, contrary to what observed for systems containing a flexible cyclohexyl *N*-substituent (**9b**, **10b**), the introduction of bulky, highly branched *N*-alkyl moieties, such as neopentyl or neophyl groups, led to strongly reduced differences between complexes with *syn* and *anti* NHC backbone configuration. Indeed, *anti* complexes **12a**,**b** showed activities only slightly higher than their *syn* congeners **11a,b** (Table S3).

Organometallics 2017, 36, 3692−3708. doi: 10.1021/acs.organomet.7b00488

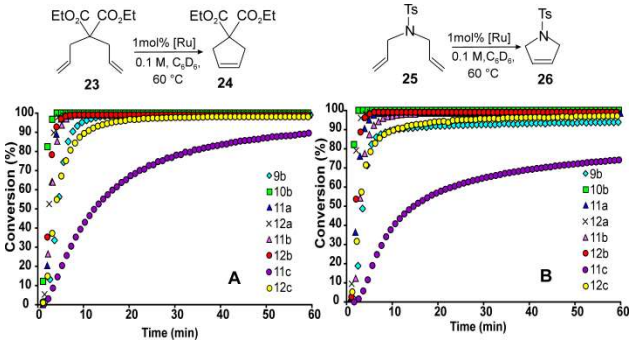

Figure 5. Kinetic profiles for the RCM of **23** (A) and **25** (B)

Increasing the steric hindrance of the *N'*-aryl substituent from 2-isopropyphenyl to mesityl group (**11c, 12c**) led to less efficient catalytic systems that, again, exhibited a significant discrepancy between catalytic behaviours of *anti* and *syn* isomers. In detail, catalysts **12c** with *anti* backbone reached almost quantitative conversion (98%) within 37 min, while *syn* **11c** did not complete the same ring-closure within 60 min (89% conversion).

In the RCM of *N*-diallyl tosylamine (**25**, Figure 5B), activities of all the tested catalytic systems were equal or inferior to those observed for the malonate derivative **23**, that typically is more reluctant to undergo cyclization reaction, confirming tendency of this class of ruthenium catalysts bearing uNHCs to give RCM nonproductive events with less demanding substrates.[12b] Steric congestion related to the presence of highly branched *N*-alkyl substituents begins to have more importance for *syn* catalysts **11a**,**b**, that were found less efficient than their *anti* counterparts. Again, a strong difference between *syn* and *anti* catalysts with *N*-cyclohexyl/*N'*-mesityl group was observed (74% and 97% conversion within 60 min for **11c** and **12c**, respectively). In both the RCM reactions, all the catalysts emerged as less active than commercial symmetrical **HGII** used at 10 times lower catalyst loading (see Table S3).

The kinetic profiles for the RCM of **27** and **29** promoted by catalysts **11a-c** and **12a-c** are sketched in Figure 6. *Anti* catalysts with neopentyl (**12a**) and neophyl *N*-substituents (**12b**) were able to quantitatively convert **27** in 13 and 10 min, respectively (Figure 6A), proving to be more efficient

Organometallics 2017, 36, 3692−3708. doi: 10.1021/acs.organomet.7b00488

than their *syn* congeners **11a** and **11b**. Moreover, a slightly major affinity of *N*-neophyl catalyst **12b** for this kind of substrate was registered (see Table S2), underlining how is not obvious to predict the effect of a structural change at the NHC on catalyst activity and how strongly this latter depends on the nature of the involved substrates. In the RCM of the *N*-tosyl derivative **29** (Figure 6B), *N*-neopentyl catalysts **11a** and **12a** showed similar activities (99% conversion within 7 and 5 minutes, respectively), whereas *N*-neophyl catalysts **11b** and **12b** disclosed a more marked reactivity difference dependent on the NHC backbone configuration. Indeed, *anti* catalyst **12b** quantitatively furnished the cyclic product **30** within 5 min, while *syn* isomer **11b** required 12 min.

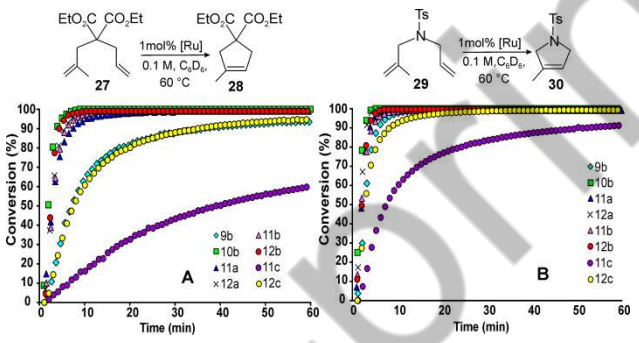

Figure 6. Kinetic profiles for the RCM of **27** (A) and **29** (B)

In both the RCM reactions for the formation of cycloolefins **28** and **30**, the worst performances were given by *N*-cyclohexyl/*N*'-mesityl catalysts, which, in addition, displayed remarkable differences in the catalytic activity of the *syn* and *anti* isomers. Indeed, as for the RCM of **27**, *anti* **12c** nearly completed cyclization (95% conversion) within 60 min, whereas only 60% conversion was reached by *syn* **11c** in the same time. In the RCM of **29**, *anti* **12c** was found able to provide quantitative conversion in 36 min, while *syn* **11c** gave 91% conversion in 60 min. Also for these transformations all the newly synthesized catalysts revealed as less efficient than **HGII** (see Table S4).

Finally, we compared the catalytic behaviors of **11a-c** and **12a-c** in the RCM of sterically demanding diolefins **31** and **33** (Figure 7, Table S5). All the catalysts were found to perform better

Organometallics 2017, 36, 3692−3708. doi: 10.1021/acs.organomet.7b00488

in the RCM of *N*-tosyl substrate **33** than in that of malonate substrate **31**. In the RCM of **33**, catalyst **12a** with a neopentyl *N*-group behaved as the best performing **10b** possessing an *N*-cyclohexyl substituent (97% conversion), while appeared less efficient in the cyclization of **31** (88% vs >97% conversion). The corresponding *syn* isomer **11a** showed lower propensity to effect both cyclizations of **31** and **33**, as also observed for the analogue *N*-cyclohexyl complex **9b**, giving **32** and **34** in 49% and 86% conversion within 60 min, respectively.

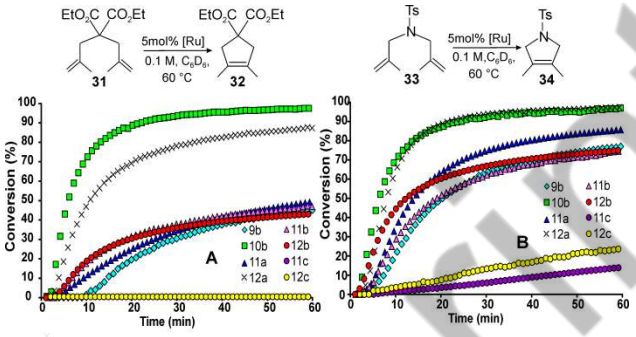

Figure 7. Kinetic profiles for the RCM of **31** (A) and **33** (B)

Moving from neopentyl to neophyl as *N*-substituent was sufficient to render negligible the role of NHC backbone configuration, indeed **11b** and **12b** exhibited comparable catalytic activities. Changing the *N'*-aromatic moiety from 2-isopropylphenyl to mesityl group dramatically affected catalytic behavior, as clearly emerged from analysis of conversion plots for both RCM reactions carried out with **11c** and **12c**. Within 60 min, **11c** and **12c** did not effect cyclization of malonate derivative **31** and gave low conversions of *N*-tosyl derivative **33 (**14% and 24%, respectively). Prolonged reaction times (see Table S3 for more details) allowed **11c** and **12c** to scarcely promote cyclization of **31** (~14% conversion) and to reach good conversions of **33** (74-94%). All the catalysts having an *N'*-2-isopropylphenyl substituent were found to exhibit better performances than **HGII** in the RCM of **31** and **33**. However, in the ring-closure of **33**, catalytic activities of **11b** and **12b** presenting a bulky neophyl *N*-substituent were very similar to that of the benchmark commercial catalyst (see Table S5).

Organometallics 2017, 36, 3692−3708. doi: 10.1021/acs.organomet.7b00488

Cross-Metathesis (CM) activity

The catalytic behavior of newly synthesized catalysts **11a-c** and **12 a-c** was then examined in the standard cross-metathesis (CM) reaction of allyl benzene (**35**) and *cis*-1,4-diacetoxy-2-butene (**36**) (Scheme 3). The results are summarized in Table 3. together with the available data for the same reactions performed with catalysts **9b**, **10b** and **HGII**.

Scheme 3. CM of substrates **35** and **36**

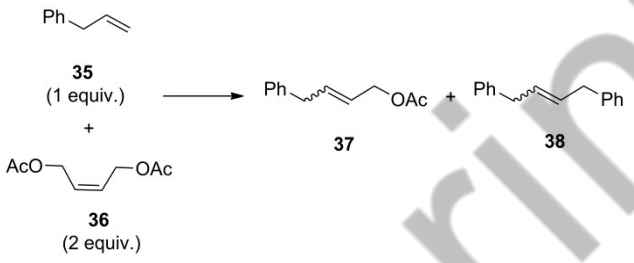

All the catalysts were found to be competent in the examined CM reaction. Replacement of a cyclohexyl group by a neopentyl or neophyl group as *N*-substituent proved to have little effect on activity and selectivity of the corresponding catalysts (entries 1-6), confirming a major tendency of complexes with *syn* backbone configuration to give lower *E/Z* ratios than their *anti* analogues[12] that indeed behave as commercial **HGII** (entry 9). On the other hand, *anti* complexes **12a,b** with highly branched *N*-alkyl groups turned out to be more able than *anti* complex **10b** to furnish the desired cross-coupling product **37** over the homocoupling product **38**. A peculiar behavior was shown by catalysts **11c** and **12c** possessing an *N'*-mesityl group (entries 7,8), for which the relative configuration of phenyls on the NHC backbone strongly differentiate yields of heterocoupled product **37** while give very similar *E/Z* ratios, underlining how catalytic efficiency is influenced by a delicate balance between NHC backbone configuration and steric features of *N*-substituents.

Organometallics 2017, 36, 3692−3708. doi: 10.1021/acs.organomet.7b00488

Table 3. CM of **35** and **36** promoted by catalysts **11a-c**, **12a-c**

entry	catalyst	**37** yield[a] (%)	E/Z[b]	**38** yield[a] (%)	E/Z[b]
1	**9b**	72	2.6	23	5.5
2	**10b**	67	7.6	28	5.7
3	**11a**	78	3.0	19	5.0
4	**12a**	80	7.6	11	6.1
5	**11b**	80	4.2	20	4.5
6	**12b**	69	7.7	7	6.6
7	**11c**	50	3.9	38	5.2
8	**12c**	89	4.4	11	5.8
9	**HGII**	69	8.6	15	5.3

[a]Isolated yield. [b]*E:Z* ratios were determined by ^{1}H NMR spectroscopy.

The increasing interest toward industrially relevant cross-metathesis reactions such as ethenolysis of fatty acid monoesters derived from renewable biomass to produce higher value-added products[3c, 3d, 3f, 22] prompted us to investigate the catalytic potential of newly developed systems in the ethenolysis of ethyl oleate (**39**, Scheme 4, Table 4). Indeed, ruthenium complexes bearing unsymmetrical NHCs have already demonstrated their attractiveness as catalysts for the cross-metathesis of methyl oleate with ethylene, showing high selectivities for ethenolysis products over self-metathesis products. [6d] This feature was attributed to their strong preference to propagate as a methylydene species.[23]

Scheme 4. Ethenolysis of ethyl oleate (**39**)

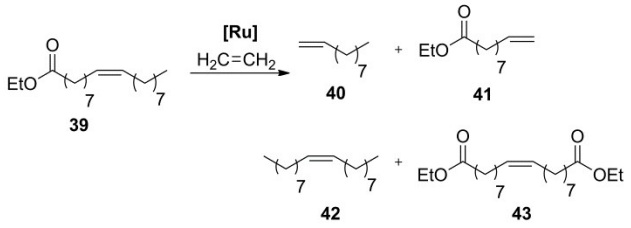

Organometallics 2017, 36, 3692−3708. doi: 10.1021/acs.organomet.7b00488

As reported in Table 4 (entries 1-12), catalysts **9b**, **10b**, **11a-c** and **12a-c** were all compared at 500 ppm catalyst loading and 10 bar of ethylene (99.9% purity). Data for the same reaction carried out in the presence of **HGII** (entry 9) were added. Moreover, comparison with **BerEt**[24a] catalyst (Figure 8), bearing a cyclic alkyl amino carbene (CAAC) ligand (entry 10), was included, since ruthenium complexes with CAAC ligands are the most active catalysts for ethenolysis known to date.[24b-f]

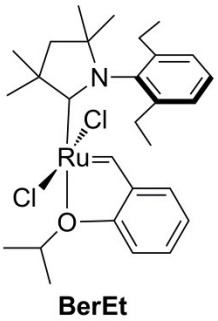

Figure 8. Ruthenium complex with a CAAC ligand (Bertrand's catalyst)

Higher selectivities, yields and turnover numbers (TONs) were displayed by catalysts with *anti* backbone configuration (entries 4, 6 ,8), which gave better performances than symmetrical **HGII** catalyst. *Anti* catalyst **10b**, although gave improved yield and TON with respect to its *syn* congener **9b** (cfr. entries 1 and 2), disclosed lower selectivity. On the other hand, catalyst **9b** was already found to show a peculiar behavior, revealing a marked propensity to give nonproductive metathesis events,[12b] which is a feature desirable for targeted reactions such as ethenolysis. The nature of the *N*-alkyl group seems to have a slight impact on the selectivity of ethenolysis reactions (entries 3-6), while sterics of the *N*-aryl substituent (mesityl versus 2-isopropylphenyl) strongly influences catalyst activity , as it is evident, above all, when catalysts **9b** , **10b** were compared with catalysts **11c** and **12c**. Indeed selectivities, yields and TONs obtained with the latter catalysts nearly equal those registered with highly performant **BerEt** catalyst (entries 7-9). In particular, **12c** showed the same selectivity as **BerEt** (83%). Encouraged by this finding, we tested catalyst **12c** also in different reaction conditions (entries 11-14). Lowering the catalyst loading to 100 ppm led to 86%

Organometallics 2017, 36, 3692−3708. doi: 10.1021/acs.organomet.7b00488

selectivity and a TON of 4100 (entry 11). When also reaction time was reduced (entry 12), 90% selectivity was achieved and yield (44) and TON (4400) were slightly improved. At 100 ppm, a lower reaction temperature (40°C) afforded lower yield and TON (entry 13), while at a catalyst loading as low as 20 ppm and 50°C (entry 14), **12c** displayed unchanged selectivity (83%) and the best TON reported so far for *N*-alkyl/*N*-aryl NHC complexes.[6d]

Table 4. Ethenolysis of ethyl oleate (**39**) with catalysts **9b**, **10b**, **11a-c** and **12a-c**.

Entry[a]	Catalyst	Cat/**39** (ppm)	Temperature (°C)	Time (h)	Conversion[b] (%)	Selectivity[c] (%)	Yield[d] (%)	TON[e]
1	**9b**	500	50	3	38	77	29	580
2	**10b**	500	50	3	63	58	36	720
3	**11a**	500	50	3	53	60	32	640
4	**12a**	500	50	3	70	64	45	900
5	**11b**	500	50	3	53	43	23	460
6	**12b**	500	50	3	71	57	40	800
7	**11c**	500	50	3	75	81	61	1220
8	**12c**	500	50	3	81	83	67	1340
9	**BertEt**	500	50	3	85	83	70	1400
10[11b]	**HovII**	500	50	3	71	43	30	600
11	**12c**	100	50	3	48	86	41	4100
12	**12c**	100	50	2	49	90	44	4400
13	**12c**	100	40	3	39	88	34	3400
14	**12c**	20	50	3	18	83	15	7500

[a]The reactions were run neat at 150 psi of ethylene (99.9% purity). [b]Conversion= 100-[(final moles of **39**) x 100/[initial moles of **39**].[c]Selectivity = 100 x (moles of ethenolysis products **40** + **41**)/[(moles of **40** + **41**) + (2 x moles of **42** + **43**)]. [d]yield= conversion x selectivity/100. [e]TON = yield x (initial moles of **39**/moles of catalyst)/100.

Organometallics 2017, 36, 3692−3708. doi: 10.1021/acs.organomet.7b00488

Asymmetric metathesis reactions

The catalytic performances of enantiomerically pure catalysts **12a-c**[25] were also evaluated in asymmetric metathesis transformations and compared to those of catalyst **10b**.[12b] The asymmetric ring-closing metahesis (ARCM) of achiral trienes **44** and **45** (Scheme 5) and the asymmetric ring-opening cross-metathesis (AROCM) of *meso*-norbornene derivative **48** with styrene (Scheme 6) were chosen as model reactions. The results are reported in Tables 5 and 6.

Scheme 5. ARCM of **44** and **45**

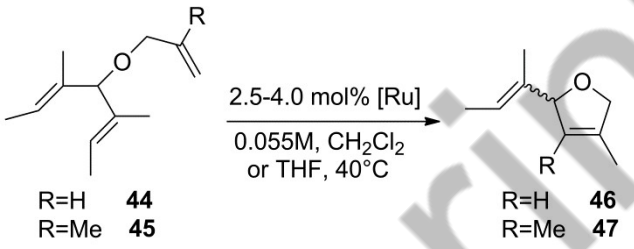

As regards the enantioselective desymmetrization of triene **44** (Table 5), the only discriminating factor for both the yield and for the enantioselectivity appeared to be the nature of the *N'*-aromatic substituent. Indeed, catalysts **12a** and **12b** containing an *N'*-2-isopropylphenyl group were able to promote the ARCM of triene **44** in high yields and low enantiomeric excesses, as already observed for the parent catalyst **10b** (entries 1, 3, 5), whereas complex **12c** with an *N*-mesityl group gave the cyclic product **46** in only 18% yield and 7% ee (entry 8). Prolonged reaction time led to almost quantitative formation of **46** (entry 9) while did not improve the enantiomeric excess. In an effort to enhance enantioselectivity, as occurred with ARCM reactions promoted by chiral systems based on C_2-symmetric NHCs,[27] the effect of using an additive such as NaI was investigated. A good increase in enantiomeric excesses was found for both **12a** and **12b** (entries 4, 6), although to a lesser extent than for **10b** (entry 2). Moreover, for **12b** the presence of NaI led to a decrease in the formation of cyclic product **46**, and also a longer reaction time resulted in comparable results in

Organometallics 2017, 36, 3692−3708. doi: 10.1021/acs.organomet.7b00488

terms of both product yield and enantioselectivity (entries 6, 7). The addition of NaI to **12c** had a deleterious effect on yield and caused inversion of enantioselectivity (entries 10, 11).

Table 5. ARCM of **44** and **45** with **10b**, **12a-c** and **2a**.

entry[a]	substrate	catalyst (mol%)	Additive	time (h)	Yield[b] (%)	ee[c] (%)
1[d]	44	**10b** (2.5)	none	2	>98	19 (*S*)
2[d]	44	**10b** (4.0)	NaI	2	>95	52 (*S*)
3	44	**12a** (2.5)	none	2	>98	16 (*S*)
4	44	**12a** (4.0)	NaI	2	>98	43 (*S*)
5	44	**12b** (2.5)	none	2	>98	18 (*S*)
6	44	**12b** (4.0)	NaI	2	83	47 (*S*)
7	44	**12b** (4.0)	NaI	20	87	43 (*S*)
8	44	**12c** (2.5)	none	2	18	7 (*R*)
9	44	**12c** (2.5)	none	41	>98	7 *(R)*
10	44	**12c** (4.0)	NaI	2	7	24 *(S)*
11	44	**12c** (4.0)	NaI	25	7	24 (*S*)
12[e]	44	**2a** (2.5)	none	2	>95	82 (S)
13[e]	44	**2a** (4.0)	NaI	2	>95	48 (S)
14[d]	45	**10b** (2.5)	none	3	>95	42 *(S)*
15[d]	45	**10b** (4.0)	NaI	3	-	-
16	45	**12a** (2.5)	none	3	>98	41 (*R*)
17	45	**12a** (4.0)	NaI	3	-	-
18	45	**12b** (2.5)	none	3	>95	36 (*S*)
19	40	**12b** (4.0)	NaI	3	-	-
20	45	**12c** (2.5)	none	3	-	-
21[f]	45	**2a** (2.5)	none		95	8 (S)

[a]Reactions without additive were performed in CH_2Cl_2; reactions with NaI were carried out in THF. [b] Yields based on NMR analysis. [c]Enantiomeric excesses determined by chiral GC. [d]Taken by ref. 12a. [e]Ref.7a. [f]Ref. 26.

In analogy with **10b** (entry 14), catalysts **12a,b** successfully accomplished the most challenging ARCM of **45** to generate tetrasubstituted olefin **47** in moderate enantiomeric excesses (entries 16,

Organometallics 2017, 36, 3692−3708. doi: 10.1021/acs.organomet.7b00488

18), while **12c** was found to be inactive. Very likely, the bulkiness of the *N'*-mesityl group reduces the active space around the metal preventing the approach of the sterically encumbered triene **45**. Attempts to improve reaction enantioselectivity using NaI as an additive failed (entries 15,17,19). As a general remark, in both the ARCM reactions, catalysts **12a-c** showed quite different behaviors from that of catalyst **2a**, representing the closest example of enantioselective catalyst with a monodentate C_1-symmetric NHC ligand.[7a] Indeed, in the ARCM of **44** they disclosed lower enantiomeric excesses and opposite response to the addition of NaI with respect to **2a** (entries 12, 13). On the other hand, they proved to be much more enantioselective than **2a** in the ARCM of **45** (entry 21).[26]

Concerning the AROCM of *cis*-5-norbornene-*endo*-2,3-dicarboxylic anhydride (**48**) with styrene (Scheme 6), all the catalysts promoted the reaction with conversions >98%, as determined by ^{1}H NMR spectroscopic analysis of crude reaction mixture after 4h. The desired product **49** was obtained in 37-57% isolated yields, along with the side products **50** and **51**, that were already observed in AROCM reactions promoted by previously reported chiral *N*-alkyl/*N*'aryl catalysts[28] (see Table 5). No other compound was detected in the reaction mixture, except stilbene deriving from the homometathesis of styrene. Moreover, only products having *trans* stereochemistry were obtained.

Scheme 6. AROCM of **48** with styrene

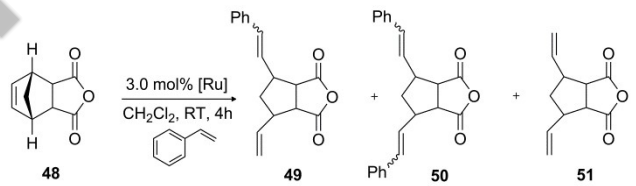

Low to moderate enantiomeric excesses were registered, and the highest ee value (43%) was achieved with catalyst **12c**, that gave also a slightly different product distribution from the catalysts

Organometallics 2017, 36, 3692−3708. doi: 10.1021/acs.organomet.7b00488

10b and **12a**,**b** (entry 4) suggesting a major propensity of **12c** to propagate *via* a methylidene species,[23] as observed in ethenolysis reaction.

Table 6. AROCM of **48** with styrene in the presence of **10b** and **12a-c**.

entry[a]	cat.	**49** yield[b] (%)	**50** yield[b] (%)	**51** yield[b] (%)	ee (**49**)[c] (%)
1[d]	**10b**	46	15	10	13
2	**12a**	57	11	16	19
3	**12b**	45	11	16	21
4	**12c**	37	16	22	43

[a]**[49]**: 0.07 M in CH_2Cl_2; 10 eq. styrene. [b]Isolated yield. [c]Enantiomeric excess determined by chiral HPLC. [b]Ref. 12b.

Conclusion

New Hoveyda-Grubbs' catalysts with unsymmetrical NHC ligands combining differently encumbered *N*-substituents and *syn* or *anti* phenyl groups on the backbone (**11a-c**, **12a-c**) have been developed. Their thermal stabilities and their catalytic behaviors were investigated, and compared to those of analogous complexes with *N*-cyclohexyl/*N'*-2-isopropylphenyl groups (**9b**, **10b**) as well as to commercially available **HGII** bearing a symmetrical NHC. *N*'-2-isopropylphenyl complexes with *anti* backbone (**10b**, **12a-c**) are more stable than their *syn* isomers (**9b**, **11a-c**), and the nature of *N*-alkyl substitution (neopentyl, neophyl vs cyclohexyl) accounts for the observed stability order. *N'*-mesityl catalysts (**11c**, **12c**) disclose outstanding stabilities that can be correlate to their higher steric bulkiness. In the RCM reactions of less encumbered substrates, the introduction of bulky, highly branched *N*-alkyl groups leads to reduced activity differences between *syn* and *anti* complexes with respect to complexes with *N*-cylohexyl group, whereas the presence of *N'*-mesityl substituent gives rise to lower activities, also correlated to the nature of NHC backbone configuration. In all the cases, catalytic performances are inferior to those of **HGII** catalyst. In the RCM of more demanding substrates, *N'*-2-isopropylphenyl *anti* catalyst with an *N*-neopentyl

Organometallics 2017, 36, 3692−3708. doi: 10.1021/acs.organomet.7b00488

substituent (**12a**) is found to be highly efficient, nearly equaling the analogous catalyst with an *N*-cyclohexyl group (**10b**), while *N'*-mesityl catalysts (**11c**, **12c**) show dramatically low activities, proving to be less efficient also than **HGII** that, as is well known, is scarcely competent to promote this class of reactions. On the other hand, catalyst **11c** and **12c** gave interesting results in the ethenolysis of ethyl oleate, outperforming their analogues and **HGII**. In particular, *anti* catalyst **12c** gives up to 90% selectivity for ethenolysis over self-metathesis products with a TON of 4400, and, at low catalyst loading (20 ppm) display 83% selectivity with a TON of 7500, that is the best result reported to date for ethenolysis reactions promoted by *N*-alkyl/*N'*-aryl NHC ruthenium catalysts. Asymmetric metathesis transformations mediated by enantiopure *anti* catalysts **12a-c** clearly indicate that the nature of the *N'*-aromatic group is the main discriminating factor for the observed activities and enantioselectivities. The strong influence of the type of NHC substitution pattern on metathesis reactions evidenced by this study underlines, once again, the importance of identifying NHC structural modifications that can allow to design of improved active and selective catalysts.

Experimental Procedure

General Information

All reactions involving organometallic compounds were performed under nitrogen using standard Schlenk and glove-box techniques. Diamines **13**[12a], **17**[12b] and **18**[12a], substrates for metathesis reactions[29] and 2-methyl-2-phenylpropanaldehyde[30] were prepared according to the literature procedures. Ethyl oleate was purchased from Sigma Aldrich Company and was and stored on activated neutral alumina before use. All other reagents were purchased from Sigma Aldrich Company and TCI chemicals and used without further purifications. Solvents were dried and distilled before use. Deuterated solvents were degassed under a N_2 flow and stored over activated 4 Å molecular sieves. Flash column chromatography of ligand intermediates were performed using silica gel 60 (230-400 mesh) from Sigma Aldrich Company and flash column chromatography of

Organometallics 2017, 36, 3692−3708. doi: 10.1021/acs.organomet.7b00488

organometallic compounds were performed, under nitrogen flow, using silica gel 60 (230-400 mesh) from TSI Cambrige. Analythical thin-layer chromatography (TLC) was performed using silica gel 60 F254 precoated plates with a fluorescent indicator. The visualization was performed using UV-light or $KMnO_4$. NMR spectra were recorded on Bruker Avance 250 spectrometer (250 MHz for ^1H; 62.5 MHz for ^{13}C), Bruker AM 300 spectrometer (300 MHz for ^1H; 75 MHz for ^{13}C), Bruker AVANCE 400 spectrometer (400 MHz for ^1H; 100 MHz for ^{13}C; 161.97 MHz for ^{31}P) and Bruker ASCEND 600 spectrometer (600 MHz for ^1H; 150 MHz for ^{13}C). NMR samples were prepared dissolving about 10 mg of compounds in 0.5 mL of deuterated solvent. ^1H and ^{13}C chemical shifts are listed in parts per million (ppm) downfield from TMS and are referenced from the solvent peaks or TMS. ^{31}P chemical shifts are referenced using H_3PO_4 as external standard. Spectra are reported as follows: chemical shift (ppm), multiplicity and integration. Multiplicity are abbreviated as follows: singlet (s), doublet (d), triplet (t), multiplet (m), broad (br), overlapped (o). Elemental analysis for C, H, N were recorded on a ThermoFinnigan Flash EA 1112 and were performed according to standard microanalytical procedures. Electrochemical measurements were conducted with an AUTOLAB PG STAT 302N potentiostat. A three-electrode configuration was employed. The working electrode was a Pt disk (diameter 2 mm), the counter-electrode a Pt bar and the reference a quasi-reference electrode (PtQRE)1, calibrated vs. octamethylferrocene as internal standard. All cyclic voltammograms were recorded in dry CH_2Cl_2 under a nitrogen atmosphere using NBu_4PF_6 (0.1 M) as supporting electrolyte at a scan rate of 100 mV/s. Potentials were referenced against the potential of octamethylferrocene. ESI-MS of organic compounds were performed on a Waters Quattro Micro triple quadrupole mass spectrometer equipped with an electrospray ion source. ESI-FT-ICR of complexes were performed on a Bruker Solaris XR. Enantiomeric excesses were determined by chiral GC (Agilent Technologies 6850) or by chiral HPLC (JASCO MD-4015 Photo diode array detector, PU4180 RMPLC Pump) and were compared

Organometallics 2017, 36, 3692−3708. doi: 10.1021/acs.organomet.7b00488

to racemic samples. Ethenolysis mixture composition was determined by GC (Agilent Technologies 7890A). Optical activity was determined using a JASCO P2000 polarimeter.

The DFT calculations were performed with the Gaussian09 set of programs,[31] using the BP86 functional of Becke and Perdew.[32] The electronic configuration of the molecular systems was described with the standard split-valence basis set with a polarization function of Ahlrichs and co-workers for H, C, N, O, and Cl (SVP keyword in Gaussian).[33] For Ru we used the small-core, quasi-relativistic Stuttgart/Dresden effective core potential, with an associated (8s7p6d)/[6s5p3d] valence basis set contracted according to a (311111/22111/411) scheme (standard SDD keywords in gaussian09).[34] The geometry optimizations were performed without symmetry constraints, and the characterization of the located stationary points was performed by analytical frequency calculations.

Synthesis of 11 a-c and 12a-c

General procedure for the arilation of diamines

Under nitrogen atmosphere, in a round bottom flask equipped with a magnetic stir and a condenser, 2,2'-bis(diphenylphosphino)-1,1'-binaphthyl (BINAP) (0.2 eq.), palladium acetate (0.1 eq.), sodium tert-butoxide (2 eq.) and toluene (C=0.05 M) were introduced. The orange solution was stirred for few minutes. Then the diamine (1 eq.) and mesityl bromide (1 eq.) were added and the reaction mixture was heated to 100 °C for 48 hours. After this time the purple mixture was cooled at room temperature, diluted with hexane and then filtered through a plug of silica gel eluting with methanol. The crude yellow oil was purified by flash column chromatography on silica gel (hexane:ethyl acetate 9:1 to 6:4) to give the desired product as a yellow oil.

14 (MW=330.5 g/mol, Yield=79%) ^{1}H NMR (300MHz, $CDCl_3$) δ: 7.29-7.27 (o m, 3H); 7.23-7.20 (o m, 3H); 7.10-7.07 (o m, 2H); 7.02-6.98 (o m, 2H); 6.75 (s, 2H); 4.43 (d, ^{3}J=4.9Hz, 1H); 4.35 (d, ^{3}J=5.2Hz, 1H); 2.21 (s, 3H); 2.16 (s, 6H). ^{13}C NMR (75MHz, $CDCl_3$) δ: 143.8; 142.8; 139.8; 130.1;

Organometallics 2017, 36, 3692−3708. doi: 10.1021/acs.organomet.7b00488

129.7; 128.5; 128.2; 128.1; 127.8; 127.2; 127.1; 67.7; 60.2; 20.6; 19.3. ESI+MS: m/z = 353.2 (MNa^+).

20 (MW=412.6 g/mol, Yield=51%) ^{1}H NMR (400MHz, $CDCl_3$) *δ*:7.20-7.15 (o m, 5H); 7.09 (br s, 3H); 7.01-6.99 (o m, 2H); 6.67 (s, 2H); 4.41 (d, ^3J=7.2Hz, 1H); 4.21 (d, ^3J=7.2Hz, 1H); 2.33-2.28 (o m, 1H); 2.15 (s, 3H); 2.13 (s, 6H); 2.01-1.98 (br d, 1H); 1.67 (br t, 3H); 1.54 (br s, 1H); 1.17-1.10 (o m, 5H). ^{13}C NMR (100MHz, $CDCl_3$) *δ:* 142.4; 142.3; 141.9; 129.8; 128.3; 128.0; 127.9; 127.8; 126.9; 67.1; 65.5; 53.7; 35.0; 32.8; 26.3; 25.2, 24.8, 20.5, 19.6. ESI+MS: m/z = 413.9 (MH^+).

$[\alpha]_D^{20}$=-45.3° (*c*=0.5, CH_2Cl_2).

General procedure for the alkylation of diamines

A round bottom flask was charged with the diamine (1 eq.), the carbonylic compound (3 eq. of pivalaldehyde for **15a** and **19a**, 6 eq. of 2-methyl-2-phenylpropanaldehyde for **15b** and **19b** and 7 eq. of cyclohexanone **15c**) and anhydrous methylene chloride (C = 0.1 M). The reaction mixture was stirred at room temperature over activated molecular sieves 4Å for 48 hours (**15a**) or 14hours (**19a**) or 5 days (**15b**, **19b** and **15c**) and then filtered. Then, the solvent was removed under reduced pressure, anhydrous MeOH was added (C=0.1 M) followed by a portionwise addition of $NaBH_4$ (4 eq.) under nitrogen atmosphere. The reaction mixture was stirred for 3.5h, diluted with methylene chloride and extracted with water. The organic layer was dried over anhydrous Na_2SO_4 and then the solvent was removed under vacuum to afford a yellowish oil which was then purified by flash column chromatography on silica gel (hexane: ethyl acetate 9:1)

15a (MW=400.6 g/mol, Yield=60%) ^{1}H NMR (300MHz, $CDCl_3$) *δ*: 7.31-7.30 (o m, 3H); 7.25-7.23 (o m, 3H); 7.19-7.16 (o m, 1H); 7.08-7.01 (o m, 3H); 6.91 (t, ^3J=8.0Hz, ^3J=7.2Hz, 1H), 6.68 (t, ^3J=7.4Hz, ^3J=7.4Hz, 1H); 6.31 (d, ^3J=8.2Hz, 1H); 5.42 (br s, 1H); 4.63 (t, ^3J=4.7Hz, ^3J=4.7Hz, 1H); 4.15 (d, ^3J=4.7Hz , 1H); 3.12-2.99 (m, 1H); 2.37 (d, ^3J=11.4Hz, 1H); 2.20 (d, ^3J=11.4Hz, 1H); 1.41 (d, ^3J=6.6Hz, 3H); 1.35 (d, ^3J=6.8Hz, 3H); 0.97 (s, 9H). ^{13}C NMR (75MHz, $CDCl_3$) *δ:* 143.9;

Organometallics 2017, 36, 3692−3708. doi: 10.1021/acs.organomet.7b00488

140.2; 139.8; 132.2; 128.2; 128.1; 127.9; 127.8; 127.4; 127.2; 126.6; 124.8; 116.9; 111.7; 68.7; 62.8; 59.8; 31.8; 27.8; 27.7; 22.5; 22.4. ESI+MS: m/z = 401.4 (MH^+).

19a (MW=400.6 g/mol, Yield=70%) ^{1}H NMR (300MHz, CD_2Cl_2) δ: 7.33-7.22 (o m, 10H); 7.15 (dd, ^3J=7.7Hz, , ^3J=1.3Hz, 1H); 6.83 (dt, ^3J=7.6Hz, ^3J=1.5Hz, 1H); 6.64 (dt, ^3J=7.0Hz, 1H); 6.21 (d, ^3J=8.1Hz, 1H); 5.82 (br s, 1H); 4.42 (d, ^3J=6.9Hz, 1H); 3.86 (d, ^3J=6.8Hz, 1H); 3.25-3.16 (m, 1H); 2.28 (d, ^3J=11.3Hz, 1H); 2.09 (d, ^3J=11.3Hz, 1H); 1.42 (d, ^3J=6.8Hz, 3H); 1.38 (d, ^3J=6.7Hz, 3H); 0.95 (s, 9H). ^{13}C NMR (75MHz, CD_2Cl_2) δ: 144.7; 142.4; 141.7; 133.2; 128.6; 128.5; 128.1; $[\alpha]_D^{20}$127.5; 127.3; 126.5; 125.0; 117.2; 111.9; 70.4; 64.4; 60.1; 31.8; 27.8; 27.7; 23.0; 22.4. ESI+MS: m/z = 401.4 (MH^+). = +49.1 (c=0.5, CH_2Cl_2).

15b (MW=462.7 g/mol, Yield=73%) ^{1}H NMR (250MHz, $CDCl_3$) δ: 7.28 (d, ^3J=4.4Hz, 4H); 7.21-7.20 (o m, 4H); 7.09-7.07 (o m, 4H);6.86 (d, ^3J=7.3Hz, 2H); 6.82-6.77 (o m, 3H); 6.60 (t, ^3J=7.5Hz, ^3J=7.3Hz, 1H); 6.19 (d, ^3J=7.9Hz, 1H); 5.12 (d, ^3J=5.1Hz, 1H); 4.43 (t, ^3J=5.2Hz, ^3J=5.1Hz, 1H); 3.99 (d, ^3J=4.9Hz, 1H); 2.90-2.82 (m, 1H); 2.62 (d, ^3J=11.3Hz, 1H); 2.51 (d, ^3J=11.3Hz, 1H); 1.37 (s, 3H); 1.31-1.29 (o m, 6H); 1.24-1.22 (d, ^3J=6.8Hz, 3H). ^{13}C NMR (100MHz, $CDCl_3$) δ: 147.7; 143.8; 140.0; 139.7; 132.2; 128.3; 128.1; 128.0; 127.9; 127.7; 127.5; 127.1; 126.5; 126.0; 125.9; 124.7; 116.9; 111.7; 68.4; 62.8; 59.8; 38.9; 27.6; 27.4; 27.0; 22.5; 22.3. ESI+MS: m/z = 463.2 (MH^+).

$[\alpha]_D^{20}$**19b**(MW=462.7 g/mol, Yield=79%) ^{1}H NMR (300MHz, $CDCl_3$) δ:7.32-7.26 (o m, 8H); 7.17-7.16 (o m 8H); 6.83 (br t, 1H); 6.64 (br t, 1H); 6.14 (d, ^3J=7.6Hz, 1H); 5.61 (br s, 1H); 4.24 (br s, 1H); 3.76 (br d, 1H); 3.05 (br t, 1H); 2.64 (d, ^3J=10.9 Hz, 1H); 2.48 (d, ^3J=10.9 Hz, 1H); 1.41-1.33 (o m, 12H). ^{13}C NMR (75MHz, $CDCl_3$) δ:147.4; 144.3; 141.8; 141.1; 132.7; 128.4; 128.2; 127.7; 127.3; 127.0; 126.4; 126.0; 124.7; 116.9; 111.7; 69.7; 64.2; 59.8; 38.8; 27.7; 27.6; 27.1; 22.8; 22.4. ESI+MS: m/z = 463.1 (MH^+). =+65.8 (c=0.5, CH_2Cl_2).

Organometallics 2017, 36, 3692−3708. doi: 10.1021/acs.organomet.7b00488

15c (MW=412.6 g/mol, Yield=50%) ^{1}H NMR (300MHz, $CDCl_3$) δ: 7.26-7.25 (o m, 3H); 7.16-7.13 (o m, 3H); 6.93-6.90 (o m, 2H); 6.85-6.82 (o m, 2H); 6.71 (s, 2H); 4.91 (br s, 1H); 4.49 (br s, 1H); 4.38 (d, ^{3}J=4.5Hz, 1H); 2.33 (br s, 1H); 2.18 (br s, 9H); 1.99 (br s, 1H); 1.71-1.57 (o m, 4H); 1.38 (br s, 1H); 1.18-1.13 (o m, 5H). ^{13}C NMR (75MHz, $CDCl_3$) δ: 142.8; 141.5; 139.7; 129.7; 129.1; 128.4; 128.0; 127.8; 127.5; 127.1; 127.0; 126.9; 66.8; 63.7; 53.2; 35.1; 33.0; 26.3; 25.1; 24.7; 20.5; 19.8. ESI+MS: m/z = 413.2 (MH^+).

General procedure for the synthesis of tetrafluoroborate salts

Diamine (1 eq.) and triethyl orthoformate (8 eq.) were introduced in a flask equipped with a magnetic stir and a condenser. The reaction mixture was stirred at room temperature for few minutes. Then ammonium tetrafluoroborate (1.2 eq.) was added and the solution was heated at 130°C for 2 hours(**16a**, **21a, 16c**, **22**) or 8 hours (**16b**, **21b**). After that, the condenser was removed in order to facilitate the evaporation of the ethanol produced during the reaction. The crude brownish oil was washed with diethyl ether and purified by flash column chromatography on silica gel (hexane:ethyl acetate 9:1 to 1:1) to obtain the product as a white solid.

16a (MW=498.4 g/mol, Yield=81%) ^{1}H NMR (400MHz, CD_2Cl_2) δ: 8.70 (s, 1H); 7.50-7.48 (o m, 2H); 7.36-7.35 (o m, 2H); 7.25-7.18 (o m, 4H); 7.11-6.97 (o m, 6H); 6.19 (br t, 1H); 5.98 (br t, 1H); 4.01 (d, ^{3}J=14.2Hz, 1H); 3.21-3.11 (o m, 2H); 1.34-1.29 (o m, 6H); 1.08 (s, 9H). ^{13}C NMR (100MHz, CD_2Cl_2) δ:160.6; 145.6; 131.8; 130.9; 130.5; 130.4; 129.8; 129.5; 129.4; 128.8; 128.7; 127.9; 127.7; 73.6; 72.2; 58.7; 33.2; 29.0; 27.7; 24.5; 24.1. ESI+MS: m/z = 411.4 ($M\text{-}BF_4^-$).

21a (MW=498.4 g/mol, Yield=90%) ^{1}H NMR (400MHz, CD_2Cl_2) δ: 8.58 (s, 1H); 7.58-7.56 (o m, 3H); 7.45-7.34 (o m, 7H); 7.27-7.25 (o m, 2H); 7.21-7.18 (o m, 2H); 5.53 (d, ^{3}J=8.0Hz, 1H); 5.37 (d, ^{3}J=8.0Hz, 1H); 3.82 (d, ^{3}J=14.9Hz, 1H); 3.06 (d, ^{3}J=14.9Hz, 1H); 2.96-2.89 (m, 1H); 1.23 (d, ^{3}J=6.8Hz, 3H); 1.09 (s, 9H); 1.02 (d, ^{3}J=6.8Hz, 3H). ^{13}C NMR (100MHz, CD_2Cl_2) δ 159.3; 145.9;

Organometallics 2017, 36, 3692−3708. doi: 10.1021/acs.organomet.7b00488

135.1; 134.7; 131.4; 131.0; 130.9; 130.8; 130.7; 130.3; 130.2; 128.8; 128.0; 127.9; 127.7; 127.6; 127.5; 127.0; 78.1; 75.4; 57.6; 33.6; 28.7; 28.0; 24.5; 23.8. ESI+MS: m/z = 411.5 ($M-BF_4^-$).

$[\alpha]_D^{20}$=+313.0 (*c*=0.5, CH_2Cl_2).

16b (MW=560.5 g/mol, Yield=71%) ^{1}H NMR (400MHz, CD_2Cl_2) *δ*: 8.36 (s, 1H); 7.41-7.32 (o m, 9H); 7.20-7.19 (o m, 4H); 7.00-6.98 (m, 3H); 6.83 (d, ^3J=6.8Hz, 3H); 5.73 (d, ^3J=12.4Hz, 1H); 4.91 (d, ^3J=11.6Hz, 1H); 4.33 (d, ^3J=14.4Hz, 1H); 3.57 (d, ^3J=14.4Hz, 1H); 3.02-2.92 (m, 1H); 1.54 (s, 3H); 1.45 (s, 3H); 1.29-1.27 (o m, 6H). ^{13}C NMR (100MHz, CD_2Cl_2) *δ* 160.1; 145.4; 145.2; 131.6; 130.9; 130.2; 129.6; 129.5; 129.2; 128.6; 127.8; 127.6; 126.4; 73.3; 71.1; 59.1; 39.8; 28.9; 27.7; 25.6; 24.5; 24.1. ESI+MS: m/z = 474.9 ($M-BF_4^-$).

21b (MW=560.5 g/mol, Yield=90%) ^{1}H NMR (300MHz, $CDCl_3$) *δ*: 8.46 (s, 1H); 7.50-7.45 (o m, 7H); 7.37-7.09 (o m, 9H); 6.97 (d, ^3J=8.3Hz, 1H); 6.81 (d, ^3J=7.6Hz, 2H); 5.00 (d, ^3J=8.3Hz, 1H); 4.60 (d, ^3J=8.0Hz, 1H); 4.30 (d, ^3J=14.8Hz, 1H); 3.55 (d, ^3J=14.8Hz, 1H); 2.67-2.56 (m, 1H); 1.57 (s, 3H); 1.40 (s, 3H); 1.15 (d, ^3J=6.7Hz, 3H); 0.86 (d, ^3J=6.9Hz, 3H). ^{13}C NMR (100MHz, CD_2Cl_2) *δ* 158.9; 145.5; 145.2; 134.9; 134.2; 130.9; 130.7; 130.4; 130.3; 129.6; 129.3; 127.9; 127.5; 127.4; 127.2; 126.8; 126.5; 73.6; 57.7; 39.6; 28.4; 28.2; 25.9; 24.7; 23.6. ESI+MS: m/z = 474.9 ($M-BF_4^-$).

$[\alpha]_D^{20}$=+210.6 (*c*=0.5, CH_2Cl_2).

16c (MW=510.4 g/mol, Yield=79%) ^{1}H NMR (300MHz, $CDCl_3$) *δ:* 8.45 (s, 1H); 7.24-7.23 (o m, 4H); 7.03-6.92 (o m, 4H); 6.85-6.72 (o m, 4H); 6.61 (d, ^3J=11.8Hz, 1H); 5.95 (d, ^3J=11.8Hz, 1H); 3.63 (t, 1H); 2.48 (s, 3H); 2.33-2.20 (o m, 4H); 2.17 (s, 3H); 1.94-1.77 (o m, 3H); 1.63-1.55 (o m, 3H); 1.38-1.21 (o m, 3H). ^{13}C NMR (100MHz, $CDCl_3$) *δ:* 157.4; 139.4; 135.2; 133.9; 131.9; 131.1; 130.3; 129.9; 129.3; 129.0; 128.9; 128.2; 127.5; 72.6; 67.8; 58.6; 32.3; 31.8; 25.3; 25.0; 24.9; 20.9; 19.7; 19.5. ESI+MS: m/z = 425.2 ($M-BF_4^-$).

Organometallics 2017, 36, 3692−3708. doi: 10.1021/acs.organomet.7b00488

$[\alpha]_D^{20}$ **22** (MW=510.4 g/mol, Yield=75%) ^{1}H NMR (250MHz, $CDCl_3$) *δ:*8.62 (s, 1H); 7.52-7.32 (o m, 7H); 7.18-7.15 (o m, 3H); 6.86 (br s, 1H); 6.69 (br s, 1H); 5.66 (d, ^3J=8.1Hz, 1H); 5.12 (d, ^3J=7.9Hz, 1H); 3.75-3.66 (br t, 1H); 2.35 (s, 3H); 2.19-2.11 (o m, 5H); 1.92-1.84 (o m, 1H); 1.75 (s, 3H); 1.63 (s, 3H); 1.45-1.20 (o m, 4H). ^{13}C NMR (100MHz, $CDCl_3$) *δ*:156.8; 140.2; 136.3; 134.8; 133.7; 130.7; 130.3; 130.2; 129.5; 129.0; 128.6; 127.0; 75.6; 70.4; 58.5; 32.3; 31.5; 25.1; 24.8; 21.0; 18.8; 18.0. ESI+MS: m/z = 424.5 ($M-BF_4^-$). =+309.8 (*c*=0.5, CH_2Cl_2).

General procedure for the synthesis of catalysts

In a glove box, potassium hexafluorotbutoxide (1 eq.) was added to a suspension of tetrafluoroborate salt (1 eq.) in toluene (C = 0.1 M). The reaction mixture was stirred for few minutes at RT and then $(PCy_3)Ru(=CH\text{-}o\text{-}OiPrC_6H_4)Cl_2$ (0.5 eq.) was added. The flask was removed from the glove box and stirred at 65°C for 2.0 hours. The reaction mixture was cooled at room temperature and purified by flash column chromatography on silica gel (hexane:diethyl ether 5:1 to 1:1).

11a (MW=730.8 g/mol, Yield=45%) ^{1}H NMR (600MHz, C_6D_6) *δ*: 16.29 (major isomer, s, 1H, Ru=CH–*o*OiPrC_6H_4); 16.22 (minor isomer, s, 0.3H); (mixed signals of both isomers) 8.96 (d, ^3J=7.3Hz, 1H); 7.99 (br s, 1H); 7.94 (br s, 1H); 7.85 (d, ^3J=6.8Hz, 1H); 7.20 (d. ^3J=7.8Hz, 1H); 7.53-7.50 (o m, 3H); 7.37 (br t, 1H); 7.31-7.28 (o m, 1H); 7.25-7.23 (br t, 1H); 7.09-7.03 (o m, 3H); 6.98 (br s, 3H); 6.93-6.90 (o m, 1H); 6.82-6.65 (o m, 5H); 6.48 (d, ^3J=9.1Hz, 1H); 6.22 (d, ^3J=7.3Hz, 1H); (only major isomer signals are shown below) 5.99 (t, ^3J=10.0Hz, 1H); 5.56 (d, ^3J=14.6Hz, 1H); 5.41 (d, ^3J=10.0Hz, 1H); 4.70(br s, 1H); 4.13 (d, ^3J=13.7Hz, 1H); 3.41 (m, 1H); 1.77 (s, 6H); 1.24 (s, 9H); 1.18 (br s, 3H). ^{13}C NMR (125MHz, C_6D_6) *δ:* (only major isomer signals are shown below) 291.8 (Ru=CH–*o*OiPrC_6H_4); 291.2; 216.1; 163.7; 163.5; 153.2; 149.1; 148.9; 148.4; 147.3; 144.5; 143.5; 142.4; 141.3; 139.7; 139.2; 138.9; 138.5; 133.8; 133.3; 133.2; 131.2; 130.7; 130.5; 130.4; 130.2; 129.6; 129.4; 129.3; 129.3; 129.0; 128.9; 128.8; 127.7; 128.6; 127.5;

Organometallics 2017, 36, 3692−3708. doi: 10.1021/acs.organomet.7b00488

127.2; 127.0; 126.9; 126.8; 126.1; 122.5; 113.2; 78.3; 77.4; 75.5; 75.2; 70.8; 69.8; 68.6; 65.2; 62.5; 62.0; 61.1; 60.2; 59.8; 32.8; 32.7; 31.3; 30.2; 29.4; 29.3; 29.2; 28.8; 27.7; 27.6; 27.3; 25.6; 24.8; 24.5; 24.4; 24.3; 24.2; 23.6; 22.8; 22.2; 22.1. Anal. Calcd. for $C_{39}H_{46}Cl_2N_2ORu$ (730.77): C, 64.10; H, 6.34; N, 3.83. Found: C, 63.88; H, 6.37; N, 3.71. ESI-FT-ICR (**11a**-Cl).: m/z = calc. 695.2342 found 695.2339 .

12a(MW=730.8 g/mol, Yield=70%) ^{1}H NMR (600MHz, C_6D_6) δ: 16.38 (minor isomer, s, 0.1H, Ru=CH–*o*OiPrC_6H_4); 16.38 (major isomer, s, 1H); (only major isomer signals are shown below) 7.75 (br s, 1H); 7.56 (d, ^3J=6.8Hz, 2H); 7.43 (d. ^3J=8.1Hz, 1H); 7.30 (t, ^3J=7.5Hz, ^3J=7.5Hz, 1H); 7.19-7.08 (o m, 5H); 7.02-6.98 (m, 3H); 6.67 (t, ^3J=7.4Hz, ^3J=7.4Hz, 1H); 6.57 (t, ^3J=7.4Hz, ^3J=7.4Hz, 1H); 6.47 (d, ^3J=8.3Hz, 1H); 5.42 (d, ^3J=13.5Hz, 1H); 5.26 (d, ^3J=2.7Hz, 1H); 4.71-4.67 (m, 1H); 4.16 (d, ^3J=14.8Hz, 1H); 3.47-3.43 (m, 1H); 1.78 (d, ^3J=6.0Hz, 3H); 1.72 (d, ^3J=6.0Hz, 3H); 1.28 (d, ^3J=7.0Hz, 3H); 1.10 (s, 9H); 0.97 (d, ^3J=7.0Hz, 3H). ^{13}C NMR (125MHz, C_6D_6) δ: (only major isomer signals are shown below) 291.7 (Ru=CH–*o*OiPrC_6H_4); 214.4; 153.6; 148.5; 144.7; 140.3; 139.6; 139.4; 133.3; 129.9; 129.7; 129.6; 129.5; 129.4; 129.0; 127.3; 127.2; 127.1; 122.8; 122.6; 113.5; 80.7; 75.4; 73.9; 63.3; 63.2; 33.9; 32.2; 29.8; 28.0; 27.9; 24.9; 24.8; 23.8; 23.7; 23.3; 22.6; 22.6; 22.4; 14.7; 14.5. Anal. Calcd. for $C_{39}H_{46}Cl_2N_2ORu$ (730.77): C, 64.10; H, 6.34; N, 3.83. Found: C, 64.12; H, 6.31; N, 3.76. ESI-FT-ICR (**12a**-Cl).: m/z = calc. 695.2342 found 695.2344 .

11b (MW=792.8 g/mol, Yield=70%) ^{1}H NMR (600MHz, C_6D_6) δ: 16.31 (major isomer, s, 1H, Ru=CH–*o*OiPrC_6H_4); 16.36 (minor isomer, s, 0.2H); (only major isomer signals are shown below) 8.88 (d, ^3J=8.3Hz, 1H); 7.50-7.47 (o m, 2H); 7.28-7.23 (o m, 1H); 7.18-7.17 (o m, 1H); 7.09-7.03 (o m, 3H); 7.01-6.95 (o m, 4H); 6.93-6.91 (o m, 1H); 6.86-6.85 (o m, 3H); 6.73-6.67 (o m, 1H); 6.59-6.56 (o m, 5H); 6.50 (d, ^3J=8.5Hz, 1H); 6.47-6.44 (o m, 1H); 5.90 (d, ^3J=9.7Hz, 1H); 5.82 (d, ^3J=13.6Hz, 1H); 5.35 (d, ^3J=7.8Hz, 1H); 4.91 (d, ^3J=9.7Hz, 1H); 4.80 (d, ^3J=13.6Hz, 1H); 4.75-

Organometallics 2017, 36, 3692−3708. doi: 10.1021/acs.organomet.7b00488

4.71 (m, 1H); 3.42-3.38 (m, 1H); 2.09 (s, 3H); 1.82-1.80 (o m, 6H); 1.45 (s, 3H); 1.20 (d, ^{3}J=7.2Hz, 3H); 1.15 (d, ^{3}J=7.2Hz, 3H). ^{13}C NMR (125MHz, C_6D_6) *δ:* (mixed signals of both isomers) 292.1; 291.6; 220.6; 215.9; 163.9; 163.7; 153.6; 149.1; 148.5; 148.3; 144.8; 144.5; 141.7; 139.5; 134.1; 133.4; 133.2; 131.4; 130.5; 130.2; 129.8; 129.7; 129.5; 129.3; 129.1; 129.0; 128.8; 128.0; 127.9; 127.9; 127.7; 127.5; 127.1; 127.0; 126.3; 126.3; 126.2; 122.8; 113.5; 78.6; 77.5; 77.4; 75.8; 75.5; 75.4; 70.2; 69.1; 68.7; 65.2; 62.7; 62.2; 61.2; 60.5; 60.1; 39.6; 39.5; 38.9; 34.0; 32.0; 30.5; 29.1; 29.0; 28.6; 28.5; 27.9; 24.8; 24.6; 24.5; 24.5; 24.4; 22.6; 22.5. Anal. Calcd. for $C_{44}H_{48}Cl_2N_2ORu$ (792.84): C, 66.66; H, 6.10; N, 3.53. Found: C, 66.70; H, 6.07; N, 3.45. ESI-FT-ICR (**11b**-Cl).: m/z = calc. 757.2499 found 757.2494 .

12b (MW=792.8 g/mol, Yield=61%) ^{1}H NMR (600MHz, C_6D_6) *δ*: 16.39 (minor isomer, s, 0.1H, Ru=CH–*o*OiPrC_6H_4); 16.36 (major isomer, s, 1H); (only major isomer signals are shown below) 7.50 (d, ^{3}J=7.6Hz, 4H); 7.19-7.15 (o m, 5H); 7.11-7.08 (o m, 3H); 7.02-6.98 (o m, 3H); 6.91 (d, ^{3}J=8.1Hz, *2*H); 6.84 (t, ^{3}J=7.6Hz, ^{3}J=7.1Hz, 1H); 6.75 (t, ^{3}J=7.6Hz, 2H); 6.68 (t, ^{3}J=7.6Hz, ^{3}J=7.1Hz, 1H); 6.50 (d, ^{3}J=8.1Hz, 1H); 5.64 (d, ^{3}J=14.2Hz, 1H); 4.79 (d, ^{3}J=14.2Hz, 1H); 4.74-4.71 (m, 1H); 4.70 (d, ^{3}J=1.9Hz, 1H); 4.60 (d, ^{3}J=1.9Hz, 1H); 3.36-3.31 (m, 1H); 2.06 (s, 3H); 1.82 (d, ^{3}J=6.2Hz, 3H); 1.78 (d, ^{3}J=6.2Hz, 3H); 1.41 (s, 3H); 1.27 (d, ^{3}J=6.6Hz, 3H); 0.89 (d, ^{3}J=6.6Hz, 3H). ^{13}C NMR (125MHz, C_6D_6) *δ:* (only major isomer signals are shown below) 291.6 (Ru=CH–*o*OiPrC_6H_4); 213.8; 153.6; 148.5; 147.7; 144.7; 139.8; 139.7; 139.5; 133.2; 129.6; 129.5; 129.5; 129.3; 129.2; 127.9; 127.3; 127.1; 126.5; 126.4; 126.2; 122.9; 122.6; 113.5; 80.4; 75.5; 72.8; 63.4; 40.0; 32.3; 32.2; 27.9; 27.8; 25.7; 24.9; 24.8; 23.6; 23.4; 22.6; 22.6; 22.5; 22.4. Anal. Calcd. for $C_{44}H_{48}Cl_2N_2ORu$ (792.84): C, 66.66; H, 6.10; N, 3.53. Found: C, 66.69; H, 6.14; N, 3.44. ESI-FT-ICR (**12b**-Cl).: m/z = calc. 757.2499 found 757.2505 .

11c (MW=742.8 g/mol, Yield=63%) ^{1}H NMR (600MHz, C_6D_6) *δ*: 16.56 (major isomer, s, 1H, Ru=CH–*o*OiPrC_6H_4); 16.44 (minor isomer, s, 0.1H); (only major isomer signals are shown below)

Organometallics 2017, 36, 3692−3708. doi: 10.1021/acs.organomet.7b00488

8.78 (br s, 1H); 7.37 (br s, 1H); 7.15-7.12 (o m, 2H); 7.00 (t, ^3J=7.5Hz, ^3J=7.5Hz, 1H); 6.78 (br s, 1H); 6.70-6.67 (o m, 5H); 6.62-6.60 (o m, 3H); 6.56 (br s, 1H); 6.47 (d, ^3J=8.3Hz, 1H); 6.27 (br s, 1H); 6.04 (d, ^3J=9.3Hz, 1H); 5.72 (t t, ^3J=3.1Hz, ^3J=3.4Hz, 1H); 5.04 (d, ^3J=9.0Hz, 1H); 4.73-4.68 (m, 1H); 3.07 (d, ^3J=11.5Hz, 1H); 2.86 (d, ^3J=12.4Hz, 1H); 2.63 (s, 3H); 2.43 (s, 3H); 1.95 (s, 3H); 1.88-1.84 (o m, 2H); 1.81 (d, ^3J=6.1Hz, 3H); 1.78 (d, ^3J=6.1Hz, 3H); 1.76-1.73 (o m, 1H); 1.67-1.59 (o m, 3H); 1.12-1.06 (o m, 1H); 0.97-0.87 (o m, 1H). ^{13}C NMR (125MHz, C_6D_6) *δ:* (only major isomer signals are shown below) 290.9 (Ru=CH–*o*OiPrC_6H_4); 214.0; 152.9; 145.0; 139.9; 138.1; 138.0; 137.5; 136.8; 133.1; 130.6; 129.6; 129.5; 129.2; 122.6; 122.5; 113.2; 75.6; 74.9; 64.9; 63.7; 33.7; 33.4; 33.3; 26.8; 26.6; 22.3; 20.8; 20.8; 20.3; 20.2. Anal. Calcd. for $C_{40}H_{46}Cl_2N_2ORu$ (742.78): C, 64.68; H, 6.24; N, 3.77. Found: C, 64.62; H, 6.27; N, 3.81. ESI-FT-ICR (**11c**-Cl).: m/z = calc. 707.2342 found 707.2339.

12c (MW=742.8 g/mol, Yield=54%) ^{1}H NMR (600MHz, C_6D_6) *δ*: 16.44 (s, 1H, Ru=CH–*o*OiPrC_6H_4); 7.14-7.08 (o m, 6H); 7.05 (t, ^3J=7.3Hz, ^3J=7.3Hz, 1H); 7.00-6.94 (o m, 5H); 6.78 (br s, 1H); 6.68 (t, ^3J=7.3Hz, ^3J=7.5Hz 1H); 6.57 (br s, 1H); 6.46 (d, ^3J=8.2Hz, 1H); 5.70 (t t, ^3J=3.1Hz, ^3J=3.0Hz, 1H); 5.48 (d, ^3J=6.4Hz, 1H); 4.78 (d, ^3J=6.8Hz, 1H); 4.71-4.67 (m, 1H); 3.10 (d, ^3J=11.1Hz, 1H); 2.85 (d, ^3J=12.4Hz, 1H); 2.54 (s, 3H); 2.07 (s, 3H); 1.96-1.88 (o m, 2H); 1.79-1.77 (o m, 9H); 1.63-1.58 (o m, 3H); 1.00-0.86 (o m, 3H). ^{13}C NMR (125MHz, C_6D_6) *δ:* 290.2 (Ru=CH–*o*OiPrC_6H_4); 211.8; 153.3; 145.2; 143.3; 141.0; 139.2; 138.8; 137.5; 130.4; 130.2; 129.7; 129.4; 129.3; 129.3; 129.1; 128.9; 122.8; 122.7; 113.5; 79.3; 75.2; 69.6; 64.2; 34.5; 34.3; 32.3; 32.2; 27.4; 26.9; 26.2; 26.1; 22.7; 22.6; 21.3; 21.2; 21.2; 21.1; 20.0; 19.9; 19.5. Anal. Calcd. for $C_{40}H_{46}Cl_2N_2ORu$ (742.78): C, 64.68; H, 6.24; N, 3.77. Found C, 64.57; H, 6.34; N, 3.68. ESI-FT-ICR (**12c**-Cl).: m/z = calc. 707.2342 found 707.2362.

General Procedures for RCM Reactions.

Organometallics 2017, 36, 3692−3708. doi: 10.1021/acs.organomet.7b00488

An NMR tube with a screw-cap septum top was charged with 0.80 mL of a solution of catalyst (1−5%) in C_6D_6. After equilibration of the sample at 60°C in the NMR probe, 0.080 mmol of substrate (0.1M) was injected into the tube. Conversions of each substrate were monitored over time by ^{1}H NMR.

*RCM of Diethyl Diallylmalonate (**23**) (Figure 5A).*

19.3 μL of **23** was injected into a heated NMR tube containing 0.80 mL of catalyst solution (1 mol %). The conversion to **24** was determined by integrating the methylene protons of the reagent at δ 2.84 (dt) and of the product at δ 3.14 (s).

*RCM of N-Tosyldiallylamine (**25**) (Figure 5B).*

17.2 μL of **25** was injected into a heated NMR tube containing 0.80 mL of catalyst solution (1 mol %). The conversion to **26** was determined by integrating the methylene protons of the reagent at δ 3.71 (d) and of the product at δ 3.90 (s).

*RCM of Diethyl Allylmethallylmalonate (**27**) (Figure 6A).*

20.5 μL of **27** was injected into a heated NMR tube containing 0.80 mL of catalyst solution (1 mol %). The conversion to **28** was determined by integrating the methylene protons of the reagent at δ 2.96(d),2.93 (s) and of the product at δ 3.18 (m), 3.07 (s)

*RCM of N-tosylallylmethallylamine (**29**) (Figure 6B).*

19.4 μL of **29** was injected into a heated NMR tube containing 0.80 mL of catalyst solution (1 mol %). The conversion to **30** was determined by integrating the methylene protons of the reagent at δ 3.70(d),3.67 (s) and of the product at δ 3.96 (m), 3.82 (s)

*RCM of Diethyl Dimethallylmalonate (**31**) (Figure 7A).*

21.6 μL of **31** was injected into a heated NMR tube containing 0.80 mL of catalyst solution (5 mol %). The conversion to **32** was determined by integrating the methylene protons of the reagent at δ 2.98(s) and of the product at δ 3.15 (s).

Organometallics 2017, 36, 3692−3708. doi: 10.1021/acs.organomet.7b00488

*RCM of N-Tosyldimethallylamine (**33**)(Figure 7B).*

20.2 μL of **33** was injected into a heated NMR tube containing 0.80 mL of catalyst solution (5 mol %). The conversion to **34** was determined by integrating the methylene protons of the reagent at δ 3.69(s) and of the product at δ 3.90 (s).

CM of allyl benzene (35) and *cis*-1,4-diacetoxy-2-butene (36) (Scheme 3, Table 3)

Under nitrogen atmosphere, 66 μL of **35** and 160 μL of **36** were added simultaneously to a solution of the catalyst (2.5 mol%) in dry methylene chloride. The reaction mixture was refluxed under nitrogen overnight and then purified on column chromatography eluting with hexane:ethyl acetate 9:1. Products **37** and **38** were obtained as transparent oils and E/Z ratios were determined by ^{1}H NMR.

Ethenolysis of 39 (Scheme 4, Table 4)

Under nitrogen atmosphere, in autoclave, **39** (5.4mmol) and dodecane (150μL) were introduced. At this point, a t=0 sample was prepared. The autoclave was purged with ethylene three times and then a toluene solution of the catalyst (20 to 500 ppm) was added. The autoclave was purged with ethylene three times and then charged with a pressure of 150psi. The reaction was stirred at 50°C or 40°C for three hours or two hours and then quenched in an ice bath. After that, ethyl vinyl ether was added and GC sample prepared in hexane. Samples were stored at -20°C until GC analysis.

ARCM of 44 and 45 without additive (Scheme 5, Table 5)

Under nitrogen atmosphere, the prochiral triene (0.11 mmol) was added to 2 mL of a CD_2Cl_2 solution of the catalyst (2.5 mol%). A portion of the reaction mixture was transferred in a NMR tube with J-young valve and heated at 40°C for two hours for substrate **44** and for three hours for the alkene **45**. Yields were determined via NMR spectroscopy of the crude product. The reaction mixture was filtered on neutral alumina and injected into GC system without further purifications.

ARCM of 44 and 45 with NaI (Scheme 5, Table 5)

Organometallics 2017, 36, 3692−3708. doi: 10.1021/acs.organomet.7b00488

Under nitrogen atmosphere, NaI (0.055 mmol) was added to 1 mL of a THF-d8 solution of the catalyst (4.0 mol%). The reaction mixture was stirred at room temperature for one hour. Then, the prochiral triene (0.055 mmol) was added and then the mixture was transferred in a NMR tube with J-young valve and heated at 40°C for two hours for substrate **39** and for three hours for the alkene **40**. Yields were determined via NMR spectroscopy of the crude product. The reaction mixture was filtered on neutral alumina and injected into GC system without further purifications.

AROCM of 48 with styrene (Scheme 6, Table 6)

Under nitrogen atmosphere, **48** (0.43 mol) and styrene (4.3 mmol) were simultaneously added to 7.5 mL of a CH_2Cl_2 solution of the catalyst (3mol%). The reaction mixture was stirred at room temperature for three hours and then concentrated and purified via column chromatography (petroleum ether:diethyl ether 1:1) to afford the product as a transparent oil. About 1.3 mg of the product was dissolved in 2 mL of hexane:2-propanol 1:1 (HPLC grade purity), filtered using a syringe filter and then injected into the HPLC system.

References

1. (a) Grela, K. *Olefin Metathesis: Theory and Practice*; John Wiley & Sons, Inc.: Hoboken, NJ, 2014.(b) Grubbs, R. H.; Wenzel, A. G.; O'Leary, D. J.; Khosravi, E. *Handbook of Metathesis, second edition*; Wiley-VCH: Weinheim, 2015.
2. (a) Scholl, M.; Ding, S.; Lee, C. W.; Grubbs, R. H. Synthesis and Activity of a New Generation of Ruthenium-Based Olefin Metathesis Catalysts Coordinated with 1,3-Dimesityl-4,5-dihydroimidazol-2-ylidene Ligands. *Org. Lett.* **1999**, *1* (6), 953-956. (b) Garber, S. B.; Kingsbury, J. S.; Gray, B. L., Hoveyda, A. H. Efficient and Recyclable Monomeric and Dendritic Ru-Based Metathesis Catalysts. *J. Am. Chem. Soc.* **2000**, *122* (34), 8168–8179. (c) Jafarpour, L.; Schanz, H. J.; Stevens, E. D.; Nolan, S. P.

Organometallics 2017, 36, 3692−3708. doi: 10.1021/acs.organomet.7b00488

Indenylidene−Imidazolylidene Complexes of Ruthenium as Ring-Closing Metathesis Catalysts. *Organometallics*, **1999**, *18* (25), 5416–5419.

3. (a) Cossy, J.; Arseniyadis, S.; Meyer, C. *Metathesis in Natural Product Synthesis*; Wiley-VCH: Weinheim, 2010. (b) Nickel, A.; Ung, T.; Mkrtumyan, G.; Uy, J.; Lee, C.; Stoianova, D.; Papazian, J.; Wei, W.-H.; Mallari, A.; Schrodi, Y.; Pederson, R. L A. Highly Efficient Olefin Metathesis Process for the Synthesis of Terminal Alkenes from Fatty Acid Esters. *Top. Catal.* **2012**, *55* (7) 518– 523. (c) Chikkali, S.; Mecking, S. Refining of Plant Oils to Chemicals by Olefin Metathesis. *Angew. Chem. Int. Ed*. **2012**, *51* (24), 5802–5808. (d) Montero de Espinosa, L.; Meier, M. A. R. Olefin Metathesis of Renewable Platform Chemicals. *Top Organomet Chem* **2012**, *39*, 1-44. (e) Higman, C. S.; Lummiss, J. A. M.; Fogg, D. E. Olefin Metathesis at the Dawn of Implementation in Pharmaceutical and Specialty-Chemicals Manufacturing . *Angew. Chem., Int. Ed.* **2016**, *55* (11) 3552– 3565. (f) Bidange, J.; Fischmeister, C.; Bruneau, C. Ethenolysis: A Green Catalytic Tool to Cleave Carbon-Carbon Double Bonds. *Chem. Eur. J.* **2016**, *22* (35), 12226 – 12244. (g) Rouen, M.; Queval, P.; Borré, E.; Falivene, L.; Poater, A.; Berthod, M.; Hugues, F.; Cavallo, L.; Baslé, O.; Olivier-Bourbigou, H.; Mauduit, M. Selective Metathesis of α-Olefins from Bio-Sourced Fischer–Tropsch Feeds. *ACS Catal.* **2016**, *6* (11) 7970– 7976.
4. (a) Vougioukalakis, G. C.; Grubbs, R. H. Ruthenium-Based Heterocyclic Carbene-Coordinated Olefin Metathesis Catalysts. *Chem. Rev.* **2010**, *110* (3), 1746-1787. (b) Samojlowicz, C.; Bieniek, M.; Grela, K. Ruthenium-Based Olefin Metathesis Catalysts Bearing N-Heterocyclic Carbene Ligands *Chem. Rev.*, **2009**, *109* (8), 3708-3742. (c) Paradiso, V.; Costabile, C.; Grisi, F. NHC backbone configuration in Ruthenium-catalyzed olefin metathesis. *Molecules* **2016**, *21* (1), 117-136.

Organometallics 2017, 36, 3692−3708. doi: 10.1021/acs.organomet.7b00488

5. (a) Tornatzky, J.; Kannenberg, A.; Blechert, S. New catalysts with unsymmetrical N-heterocyclic carbene ligands. *Dalton Trans.* **2012**, *41* (27), 8215-8225. (b) Hamad, F. B.; Sun, T.; Xiao, S.; Verpoort, F. Olefin metathesis ruthenium catalysts bearing unsymmetrical heterocylic carbenes. *Coord. Chem. Rev.* **2013**, *257* (15-16), 2274-2292. (c) Shahane, S.; Bruneau, C.; Fischmeister, C. Z Selectivity: Recent Advances in one of the Current Major Challenges of Olefin Metathesis. *ChemCatChem* **2013**, *5* (12), 3436-3459 (f) Montgomery, T. P.; Johns, A. M.; Grubbs, R. H. Recent Advancements in Stereoselective Olefin Metathesis Using Ruthenium Catalysts. *Catalysts* **2017**, *7* (3), 87-124.

6. Selected examples of *N*-alkyl/*N*-aryl NHC-Ru complexes: (a) Dinger, M. B.; Nieczypor, P.; Mol, J. C. Adamantyl-Substituted N-Heterocyclic Carbene Ligands in Second-Generation Grubbs-Type Metathesis Catalysts. *Organometallics* **2003**, *22* (25), 5291-5296. (b) Vehlow, K; Maechling, S.; Blechert, S. Ruthenium Metathesis Catalysts with Saturated Unsymmetrical N-Heterocyclic Carbene Ligands. *Organometallics* **2006**, *25* (1), 25-28. (c) Ledoux, N.; Allaert, B.; Pattyn, S.; Mierde, H. V.; Vercaemst, C.; Verpoort, F. N,N′-Dialkyl- and N-Alkyl-N-mesityl-Substituted N-Heterocyclic Carbenes as Ligands in Grubbs Catalysts. *Chem. Eur. J.* **2006**, *12* (17), 4654-4661 (d) Thomas, R. M.; Keitz, B. K.; Champagne, T. M.; Grubbs, R. H. Highly Selective Ruthenium Metathesis Catalysts for Ethenolysis. *J. Am. Chem. Soc.* **2011**, *133* (19), 7490-7496. (e) Ablialimov, O.; Kędziorek, M.; Torborg, C.; Malińska, M.; Woźniak, K.; Grela, K. New Ruthenium(II) Indenylidene Complexes Bearing Unsymmetrical N-Heterocyclic Carbenes. *Organometallics* **2012**, *31* (21), 7316−7319. (f) Rouen, M.; Borre, E.; Falivene, L.; Toupet, L.; Berthod, M.; Cavallo, L.; Olivier-Bourbigou, H.; Mauduit, M. Cycloalkyl-based unsymmetrical unsaturated (U2)-NHC ligands: flexibility and dissymmetry in ruthenium-catalysed olefin metathesis. *Dalton Trans*. **2014**, *43* (19), 7044-7049; (g) Yu, B.; Hamad, F. B.; Sels, B.; Van Hecked, K.;

Organometallics 2017, 36, 3692−3708. doi: 10.1021/acs.organomet.7b00488

Verpoort, F. Ruthenium indenylidene complexes bearing N-alkyl/N-mesityl-substituted N-heterocyclic carbene ligands. *Dalton Trans.*, **2015**, *44* (26), 11835-11842.

7. (a) Van Veldhuizen, J.J.; Gillingham, D.G.; Garber, S.B.; Kataoka, O.; Hoveyda, A.H. Chiral Ru-Based Complexes for Asymmetric Olefin Metathesis: Enhancement of Catalyst Activity through Steric and Electronic Modifications. *J. Am. Chem. Soc.* **2003**, *125* (41), 12502–12508. (b) Fournier, P.-A.; Collins, S. K. A Highly Active Chiral Ruthenium-Based Catalyst for Enantioselective Olefin Metathesis. *Organometallics* **2007**, *26* (12), 2945-2949. (c) Tiede, S.; Berger, A.; Schlesiger, D.; Rost, D.; Lühl, A.; Blechert, S. Highly Active Chiral Ruthenium-Based Metathesis Catalysts through a Monosubstitution in the N-Heterocyclic Carbene. *Angew. Chem., Int. Ed.* **2010**, *49* (23), 3972-3975. (d) Hartung, J.; Dornan, P.K.; Grubbs, R.H. Enantioselective Olefin Metathesis with Cyclometalated Ruthenium Complexes. *J. Am. Chem. Soc.* **2014**, *136* (37), 13029-13037.
8. (a) Vehlow, K.; Wang, D.; Buchmeiser, M. R.; Blechert, S. Alternating Copolymerizations Using a Grubbs-Type Initiator with an Unsymmetrical, Chiral N-Heterocyclic Carbene Ligand. *Angew. Chem. Int. Ed.* **2008**, *47* (14), 2615-2618. (b) Engl, P. S.; Fedorov, A.; Coperet, C.; Togni, A. N-Trifluoromethyl NHC Ligands Provide Selective Ruthenium Metathesis Catalysts. *Organometallics* **2016**, *35* (6), 887-893.
9. Kavitake, S.; Samantaray, M. K.; Dehn, R.; Deuerlein, S.; Limbach, M.; Schachner, J. A.; Jeanneau, E.; Copéret, C.; Thieuleux, C. Unsymmetrical Ru-NHC catalysts: a key for the selective tandem Ring Opening–Ring Closing alkene Metathesis (RO–RCM) of cyclooctene. *Dalton Trans.* **2011**, *40* (46), 12443-12446.
10. Herbert, M. B.; Grubbs, R. H. Z-Selective Cross Metathesis with Ruthenium Catalysts: Synthetic Applications and Mechanistic Implications. *Angew. Chem. Int. Ed.* **2015**, *54* (17), 5018-5024.

Organometallics 2017, 36, 3692−3708. doi: 10.1021/acs.organomet.7b00488

11. (a) Ablialimov, O.; Kędziorek, M.; Malińska, M.; Woźniak, K.; Grela, K. Synthesis, Structure, and Catalytic Activity of New Ruthenium(II) Indenylidene Complexes Bearing Unsymmetrical N-Heterocyclic Carbenes. *Organometallics* **2014**, *33* (9) 2160-2171. (b) Smoleń, M.; Kośnik, W.; Loska, R.; Gajda, R.; Malińska, M.; Woźniak, K.; Grela, K. Synthesis and catalytic activity of ruthenium indenylidene complexes bearing unsymmetrical NHC containing a heteroaromatic moiety. *RSC Adv*., **2016**, *6* (80), 77013-77019.
12. (a) Paradiso, V.; Bertolasi, V.; Grisi, F. Novel Olefin Metathesis Ruthenium Catalysts Bearing Backbone Substituted Unsymmetrical NHC Ligands. *Organometallics* **2014**, *33* (21), 5932-5935. (b) Paradiso, V.; Bertolasi, V.; Costabile, C.; Grisi, F. Ruthenium olefin metathesis catalysts featuring unsymmetrical N-heterocyclic carbenes. *Dalton Trans.* **2016**, *45* (2), 561-571.
13. Parsons,S.; Flack, H.; Wagner,T. Use of intensity quotients and differences in absolute structure refinement. *Acta Crystallogr.* **2013**, B69, 249-259.
14. Burnett M. N.; Johnson, C. K. ORTEP III, Report ORNL-6895, Oak Ridge National Laboratory, Oak Ridge, TN, **1996**.
15. Dichloro[1,3-bis(2,4,6-trimethylphenyl)-2-imidazolidinylidene](2-isopropoxyphenyl methylene)ruthenium(II) (**HGII**)
16. In the employed conditions, after one month 100% of **11c** and **12c** still persisted, while 79% of **HGII** was undecomposed.
17. Małecki, P.; Gajda, K.; Ablialimov, O.; Malińska, M.; Gajda, R.; Woźniak, K.; Kajetanowicz, A.; Grela, K. Hoveyda-Grubbs Type Precatalysts with Unsymmetrical N-Heterocyclic Carbenes as Effective Catalysts in Olefin Metathesis. *Organometallics* **2017**, *36* (11), 2153-2166.

Organometallics 2017, 36, 3692−3708. doi: 10.1021/acs.organomet.7b00488

18. Wu. M, M.; Gill, A. M. ; Yunpeng, L.; Falivene, L.; Yongxin, L.; Ganguly, R.; Cavallo, L.; Garcìa, F. Synthesis, structural studies and ligand influence on the stability of aryl-NHC stabilized trimethylaluminium complexes. *Dalton Trans.* **201**5, *44* (34), 15166-15174.

19. Falivene, L.; Credendino, R.; Poater, A.; Petta, A.; Serra, L.; Oliva, R.; Scarano, V.; Cavallo, L. SambVca 2. A Web Tool for Analyzing Catalytic Pockets with Topographic Steric Maps. *Organometallics* **2016**, *35* (13), 2286–2293.

20. Süßner, M.; Plenio, H. π-Face donor properties of N-heterocyclic carbenes. *Chem. Commun.* **2005**, (43), 5417-5419.

21. Perfetto, A.; Bertolasi, V.; Costabile, C.; Paradiso, V.; Caruso, T.; Longo, P.; Grisi, F. Methyl and Phenyl Substituent Effects on the Catalytic Behavior of NHC Ruthenium Complexes. *RSC Adv.* **2016**, *6* (98), 95793-95804.

22. (a) Mol, J. C. Application of olefin metathesis in oleochemistry: an example of green chemistry. *Green Chemistry* **2002**, *4* (1), 5-13. (b) Spekreijse, J.; Sanders, J. P. M.; Bitter, J. H.; Scott, E. L. The Future of Ethenolysis in Biobased Chemistry. *ChemSusChem* **2017**, *10* (3) ,470-482.

23. (a) Stewart, I. C.; Keitz, B. K.; Kuhn, K. M.; Thomas, R. M.; Grubbs, R. H. Nonproductive Events in Ring-Closing Metathesis Using Ruthenium Catalysts. *J. Am. Chem. Soc.* **2010**, *132* (25), 8534-8535. (b) Keitz, B. K.; Grubbs, R. H. Probing the Origin of Degenerate Metathesis Selectivity via Characterization and Dynamics of Ruthenacyclobutanes Containing Variable NHCs. *J. Am. Chem. Soc.* **2011**, *133* (40), 16277–16284.

24. (a) Anderson, D. R.; Lavallo, V.; O'Leary, D. J.; Bertrand, G.; Grubbs, R. H. Synthesis and reactivity of olefin metathesis catalysts bearing cyclic (alkyl)(amino)carbenes. *Angew. Chem. Int. Ed.* **2007**, *46* (38) , 7262-7265. (b) Anderson, D. R.; Ung, T.; Mkrtumyan, G.; Bertrand, G.; Grubbs, R. H. Kinetic Selectivity of Olefin Metathesis Catalysts Bearing

Organometallics 2017, 36, 3692−3708. doi: 10.1021/acs.organomet.7b00488

Cyclic (Alkyl)(Amino)Carbenes. *Organometallics* **2008**, *27* (7), 563-566. (c) Schrodi, Y.; Ung, T.; Vargas, A.; Mkrtumyan, G.; Lee, W.-C.; Champagne, T. M.; Pederson, R. L.; Hong, S. H. Ruthenium Olefin Metathesis Catalysts for the Ethenolysis of Renewable Feedstocks. *Clean* **2008**, *36* (8), 669-673. (d) Zhang, J.; Song, S.; Wang, X.; Jiao, J.; Shi, M. Ruthenium-catalyzed olefin metathesis accelerated by the steric effect of the backbone substituent in cyclic (alkyl)(amino) carbenes. *Chem. Commun.* **2013**, **49**, 9491-9493. (e) Marx, V. M.; Sullivan, A. H.; Melaimi, M.; Virgil, S. C.; Keitz, B. K.; Weinberger, D. S.; Bertrand, G.; Grubbs, R. H. Cyclic alkyl amino carbene (CAAC) ruthenium complexes as remarkably active catalysts for ethenolysis. *Angew. Chem. Int. Ed.* **2015**, *54* (6), 1919-1923. (f) Gawin, R.; Kozakiewicz, A;. Guńka, P. A.; Dąbrowski, P.; Skowerski, K. Bis(Cyclic Alkyl Amino Carbene) Ruthenium Complexes: A Versatile, Highly Efficient Tool for Olefin Metathesis. *Angew. Chem. Int. Ed.* **2017**, *56* (4), 981-986.

25. Only enantiopure *anti* catalysts were tested due to the difficulty to separate racemic mixtures of *syn* isomers, although preliminary studies to evaluate the effect of *syn* and *anti* stereochemical relationships of substituents on the backbone of uNHC have been undertaken by some of us (see Paradiso, V.; Menta, S.; Pierini, M.; Della Sala, G.; Ciogli, A.; Grisi, F. Enantiopure C1-symmetric N-Heterocyclic Carbene Ligands from desymmetrized meso-1,2-Diphenylethylenediamine: Application in Ruthenium- Catalyzed Olefin Metathesis. *Catalyst*s **2016**, *6* (11), 177).
26. Stenne, B.; Timperio, J.; Savoie, J.; Dudding, T.; Collins, S. K. Desymmetrizations Forming Tetrasubstituted Olefins Using Enantioselective Olefin Metathesis. *Org. Lett.* **2010**, *12* (9), 2032–2035.
27. (a) Seiders, T. J.; Ward, D. W.; Grubbs, R. H. Enantioselective Ruthenium-Catalyzed Ring-Closing Metathesis. *Org. Lett.*, **2001**, *3* (20), 3225-3228. (b) Funk, T. W.; Berlin, J. M.;

Organometallics 2017, 36, 3692−3708. doi: 10.1021/acs.organomet.7b00488

Grubbs, R. H. Highly Active Chiral Ruthenium Catalysts for Asymmetric Ring-Closing Olefin Metathesis. *J. Am. Chem. Soc.*, **2006**, *128* (6), 1840-1846.

28. Thomas, R. M.; Grubbs, R. H. Mechanistic Studies of Enantioselective N-aryl, N-alkyl NHC Ruthenium Metathesis Catalysts in Asymmetric Ring-Opening Cross-Metathesis. *Chem. New Zealand* **2011**, *75* (2), 65-71.
29. M. Gatti, L. Vieille Petit, L. Xinjun, R. Mariz, E. Drinkel, A. Linden, R. Dorta Impact of NHC Ligand Conformation and Solvent Concentration on the Ruthenium-Catalyzed Ring-Closing Metathesis Reaction. *J. Am. Chem. Soc.* **2009**, *131* (27), 9498-9499.
30. C.A.B. Rodrigues, M. Norton de Matos, B.M.H. Guerreiro, A.M.L. Gonçalves, C.C. Romão, C.A.M. Afonso Water as efficient medium for mild decarbonylation of tertiary aldehydes. *Tetrahedron Letters* **2011***, 52* (22)*,* 2803-2807.
31. 30 Gaussian 09, Revision A.02, Frisch, M. J.; Trucks, G. W.; Schlegel, H. B.; Scuseria, G. E.; Robb, M. A.; Cheeseman, J. R.; Scalmani, G.; Barone, V.; Mennucci, B.; Petersson, G. A.; Nakatsuji, H.; Caricato, M.; Li, X.; Hratchian, H. P.; Izmaylov, A. F.; Bloino, J.; Zheng, G.; Sonnenberg, J. L.; Hada, M.; Ehara, M.; Toyota, K.; Fukuda, R.; Hasegawa, J.; Ishida, M.; Nakajima, T.; Honda, Y.; Kitao, O.; Nakai, H.; Vreven, T.; Montgomery, J. A., Jr.; Peralta, J. E.; Ogliaro, F.; Bearpark, M.; Heyd, J. J.; Brothers, E.; N. Kudin, K.; Staroverov, V. N.; Kobayashi, R.; Normand, J.; Raghavachari, K.; Rendell, A.; Burant, J. C.; Iyengar, S. S.; Tomasi, J.; Cossi, M.; Rega, N.; Millam, J. M.; Klene, M.; Knox, J. E.; Cross, J. B.; Bakken, V.; Adamo, C.; Jaramillo, J.; Gomperts, R.; Stratmann, R. E.; Yazyev, O.; Austin, A. J.; Cammi, R.; Pomelli, C.; Ochterski, J. W.; Martin, R. L.; Morokuma, K.; Zakrzewski, V. G.; Voth, G. A.; Salvador, P.; Dannenberg, J. J.; Dapprich, S.; Daniels, A. D.; Farkas, O.; Foresman, J. B.; Ortiz, J. V.; Cioslowski, J.; Fox, D. J. Gaussian, Inc., Wallingford CT, **2009**.

Organometallics 2017, 36, 3692−3708. doi: 10.1021/acs.organomet.7b00488

32. Becke, A. D. Density-functional exchange-energy approximation with correct asymptotic behavior. *Phys. Rev. A* **1988**, *38* (6), 3098-3100. b) Perdew, J. P. Density-functional approximation for the correlation energy of the inhomogeneous electron gas. *Phys. Rev. B* **1986**, *3*3 (12), 8822-8824. c) Perdew, J. P. Density-functional approximation for the correlation energy of the inhomogeneous electron gas. *Phys. Rev. B* **1986**, *34* (13), 7406-7406.

33. Schaefer, A., Horn, H. and Ahlrichs, R. *J.* Fully optimized contracted Gaussian basis sets for atoms Li to Kr. *Chem. Phys.* 1992, *97*(4), 2571– 2577.

34. (a) Haeusermann, U., Dolg, M., Stoll, H. and Preuss, H. Accuracy of energy-adjusted quasirelativistic ab initio pseudopotentials: all-electron and pseudopotential benchmark calculations for Hg, HgH and their cations. *Mol. Phys.* **1993**, *78* (5), 1211– 1224. b) Kuechle, W., Dolg, M., Stoll, H. and Preuss, H. *J.* Energy-adjusted pseudopotentials for the actinides. Parameter sets and test calculations for thorium and thorium monoxide.*Chem. Phys.* **1994**, *100* (10), 7535– 7542. c) Leininger, T., Nicklass, A., Stoll, H., Dolg, M. and Schwerdtfeger, P. The accuracy of the pseudopotential approximation. II. A comparison of various core sizes for indium pseudopotentials in calculations for spectroscopic constants of InH, InF, and InCl *J. Chem. Phys.* **1996**, 105 (3), 1052– 1059.

Notes

Electronic Supplementary Information (ESI) available: Experimental procedures, figures giving NMR spectra of the new complexes, GC and HPLC chromatograms of ethenolysis reaction mixture, **46**, **47** and **49**, tables and CIF files giving experimental details for complexes **47** and **48**, and Cartesian coordinates for the optimized structures.

Organometallics 2017, 36, 3692−3708. doi: 10.1021/acs.organomet.7b00488

Acknowledgements

The authors thank Dr Patrizia Iannece, Dr Ivano Immediata, Patrizia Oliva for technical assistance. This work was financed by the Ministero dell'Università e della Ricerca Scientifica e Tecnologica. Financial support from POR CAMPANIA FESR 2007/2013 O.O.2.1.-CUP B46D14002660009 "Il potenziamento e la riqualificazione del sistema delle infrastrutture nel settore dell'istruzione, della formazione e della ricerca" is gratefully acknowledged. M.D. and K.G. acknowledge the National Science Centre (Poland) for the NCN MAESTRO Grant No. DEC-2012/04A/ST5/00594.

Organometallics 2017, 36, 3692−3708. doi: 10.1021/acs.organomet.7b00488

TOC